IEEE Access
Multidisciplinary | Rapid Review | Open Access Journal

Received November 30, 2018, accepted January 1, 2019, date of publication February 11, 2019, date of current version March 29, 2019.

Digital Object Identifier 10.1109/ACCESS.2019.2898767

A Comprehensive Analysis of the Achievable Channel Capacity in $\mathcal{F}$ Composite Fading Channels

SEONG KI YOO[1], (Member, IEEE), PASCHALIS C. SOFOTASIOS[2,3], (Senior Member, IEEE), SIMON L. COTTON[1], (Senior Member, IEEE), SAMI MUHAIDAT[2,4], (Senior Member, IEEE), F. JAVIER LOPEZ-MARTINEZ[5], (Senior Member, IEEE), JUAN M. ROMERO-JEREZ[6], (Senior Member, IEEE), AND GEORGE K. KARAGIANNIDIS[7], (Fellow, IEEE)

[1]Center for Wireless Innovation, ECIT Institute, Queen's University Belfast, Belfast BT3 9DT, U.K.
[2]Center for Cyber-Physical Systems, Department of Electrical and Computer Engineering, Khalifa University, Abu Dhabi 127788, United Arab Emirates
[3]Department of Electrical Engineering, Tampere University, 33101 Tampere, Finland
[4]Institute for Communication Systems, University of Surrey, Guildford GU2 7XH, U.K.
[5]Departmento de Ingenieria de Comunicaciones, Universidad de Málaga-Campus de Excelencia Internacional Andalucia Tech., 29071 Málaga, Spain
[6]Departmento de Tecnologia Electronica, Universidad de Málaga-Campus de Excelencia Internacional Andalucia Tech., 29071 Málaga, Spain
[7]Department of Electrical and Computer Engineering, Aristotle University of Thessaloniki, 54124 Thessaloniki, Greece

Corresponding author: Paschalis C. Sofotasios (p.sofotasios@ieee.org)

This work was supported in part by the U.K. Engineering and Physical Sciences Research Council under Grant EP/L026074/1, in part by the Department for the Economy Northern Ireland under Grant USI080, and in part by the Khalifa University under Grant KU-8474000122 and Grant KU-8474000137.

ABSTRACT The $\mathcal{F}$ composite fading model was recently proposed as an accurate and tractable statistical model for the characterization of the composite fading conditions encountered in realistic wireless communication scenarios. In the present contribution, we capitalize on the distinct properties of this composite model to derive an analytical framework and then to evaluate the achievable channel capacity over $\mathcal{F}$ composite fading channels under different channel state information (CSI) assumptions. To this end, we first consider that the CSI is known only at the receiver, for which we derive novel analytic expressions for the channel capacity under optimum rate adaptation as well as for the corresponding effective capacity. Then, by considering that the CSI is known both at the transmitter and at the receiver, we derive novel analytic expressions for the channel capacity under optimum power and rate adaptation, channel inversion with fixed rate and truncated channel inversion with fixed rate. The derived analytic expressions for the considered scenarios are provided in closed-form and benefit from being tractable both analytically and numerically. This enables the derivation of simple bounds as well as approximate and asymptotic expressions, which are shown to be useful as they provide meaningful insights on the effect of fading conditions and/or latency on the overall system performance.

INDEX TERMS Channel capacity, channel state information, composite fading channel, effective capacity.

I. INTRODUCTION

It is well-known that wireless transmission is subject to multipath fading which is mainly caused by the constructive and destructive interference between two or more versions of the transmitted signal. Since multipath fading is typically detrimental to the performance of wireless communications systems, it is important to characterize and model multipath fading channels accurately in order to understand and improve their behavior. In this context, numerous fading models such as Rayleigh, Rice and Nakagami-*m* have been utilized in an attempt to characterize multipath fading, depending on the nature of the radio propagation environment [1]–[4].

Based on the above, extensive analyses on the performance of various wireless communication systems have been reported in [5]–[14] and the references therein. Specifically, the authors in [5]–[7] introduced the concepts of capacity

The associate editor coordinating the review of this manuscript and approving it for publication was Shree Krishna Sharma.

analysis under different adaptation policies and carried out an extensive analysis over Rayleigh and Nakagami-*m* fading channels. Likewise, the ergodic capacity over correlated Rician fading channels and under generalized fading conditions was investigated in [8] and [9], respectively. In the same context, comprehensive capacity analyses over independent and correlated generalized fading channels were performed in [10]–[12] for different diversity receiver configurations. Also, a lower bound for the ergodic capacity of distributed multiple input multiple output (MIMO) systems was derived in [13], while the effective throughput over generalized multipath fading in multiple input single output (MISO) systems was analyzed in [14].

In most practical wireless scenarios, the transmitted signal may not only undergo multipath fading, but also simultaneous shadowing. Shadowing can be typically modeled with the aid of lognormal, gamma, inverse Gaussian and inverse gamma distributions [15]–[20]. Following from this, the simultaneous occurrence of multipath fading and shadowing can be taken into account using any one of the composite fading models, introduced in the open technical literature [21]–[28]. Capitalizing on this, the performance of digital communications systems over composite fading channels has been analyzed in [29]–[48]. The majority of these contributions are concerned with analyses relating to outage probability and error analyses in conventional and diversity based communication scenarios. However, a corresponding analysis of the channel capacity has only been partially addressed. Furthermore, many of the existing studies are either limited to an ergodic capacity analysis for the case of independent and correlated fading channels in conventional, relay and multi-antenna communication scenarios or to the effective capacity and channel capacity under different adaptation policies for the case of conventional communication scenarios. In addition, these analyses have been comprehensively addressed only for the case of gamma distributed shadowing and partially for composite models based on lognormal or IG shadowing effects.

Motivated by this, the authors in [49] recently proposed the use of the Fisher-Snedocor $\mathcal{F}$ distribution to describe the composite fading conditions encountered during realistic wireless transmission. This composite model is based on the key assumption that the root mean square (rms) power of a Nakagami-*m* signal is subject to variation induced by an inverse Nakagami-*m* random variable (RV). It was shown in [49] that this assumption renders the $\mathcal{F}$ fading model capable of providing a better fit to measurement data than the widely used generalized-*K* fading model. Additionally, the algebraic representation of the $\mathcal{F}$ composite fading distribution is fairly tractable and simpler than that of the generalized-*K* distribution, which until now has largely been considered the most analytically tractable composite fading model.

As a result, this model is characterized by its distinct combination of accurate modeling capability and algebraic tractability. In the present contribution, a comprehensive framework for the capacity analysis over $\mathcal{F}$ composite fading channels is provided. The main contributions of the this paper are summarized below:

- We derive additional analytic expressions for the key statistical metrics of the $\mathcal{F}$ composite fading model. These formulations are generic and thus, well suited to information-theoretic analyses, such as those in the present contribution.
- We quantify the channel capacity under $\mathcal{F}$ composite fading conditions assuming that CSI is known only at the receiver. Based on this, we derive novel exact closed-form expressions for the corresponding channel capacity with optimum rate adaptation (C_{ORA}) and effective capacity (C_{eff}) measures.
- Capitalizing on the above, we derive accurate approximations and tight bounds for the considered (C_{ORA}) and effective capacity (C_{eff}) measures. These expressions are particularly simple and provide useful theoretical and practical insights into the impact of multipath fading and shadowing on the overall system performance.
- We quantify the channel capacity under $\mathcal{F}$ composite fading conditions assuming that CSI is known both at the transmitter and at the receiver. Based on this, we derive novel exact closed-form expressions for the corresponding channel capacity with optimum power and rate adaptation (C_{OPRA}), the channel inversion and fixed rate (C_{CIFR}) and the truncated channel inversion and fixed rate (C_{TIFR}).
- Based on the above, we then derive accurate approximations and tight bounds for the considered cases, which are rather simple and insightful.
- We also derive analytic expressions for the optimum cut-off SNR (γ_0) for the considered C_{OPRA} case.
- We utilize all of these results to provide a quantification of the channel capacity limits for different fading conditions. This provides numerous insights which are expected to be useful in the design and deployment of communication systems in the context of emerging wireless applications, such as body area networks and vehicular communications, to name but a few.

The remainder of the paper is organized as follows: In Section II, we briefly review and redefine the $\mathcal{F}$ composite fading model. Then an analytical framework for the capacity analysis over $\mathcal{F}$ composite fading channels is derived in Section III. Section IV provides some numerical results while Section V presents some concluding remarks.

II. THE $\mathcal{F}$ COMPOSITE FADING MODEL

Similar to the physical signal model proposed for the Nakagami-*m* fading channel [50], the received signal in an $\mathcal{F}$ composite fading channel is composed of separable clusters of multipath in which the scattered waves have similar delay times, with the delay spreads of different clusters being relatively large. However, in contrast to the Nakagami-*m* signal, in an $\mathcal{F}$ composite fading channel, the rms power of the

received signal is subject to random variation induced by shadowing. Based on this, the received signal envelope, R, can be expressed as

$$R = \sqrt{\sum_{i=1}^{m} \alpha^2 I_i^2 + \alpha^2 Q_i^2}, \tag{1}$$

where m represents the number of clusters of multipath, I_i and Q_i are independent Gaussian RVs which denote the in-phase and quadrature phase components of the multipath cluster i, respectively, where

$$\mathbb{E}[I_i] = \mathbb{E}[Q_i] = 0 \tag{2}$$

and

$$\mathbb{E}[I_i^2] = \mathbb{E}[Q_i^2] = \sigma^2, \tag{3}$$

with $\mathbb{E}[\cdot]$ denoting statistical expectation. In (1), α is a normalized inverse Nakagami-m RV where m_s is the shape parameter and $\mathbb{E}[\alpha^2] = 1$, such that

$$f_\alpha(\alpha) = \frac{2(m_s-1)^{m_s}}{\Gamma(m_s)\,\alpha^{2m_s+1}} \exp\left(-\frac{m_s-1}{\alpha^2}\right), \tag{4}$$

where $\Gamma(\cdot)$ represents the gamma function [51, eq. (8.310.1)].

Following the approach in [49], we can obtain the corresponding PDF[1] of the received signal envelope, R, in an $\mathcal{F}$ composite fading channel, namely

$$f_R(r) = \frac{2\,m^m (m_s-1)^{m_s}\,\Omega^{m_s} r^{2m-1}}{B(m,m_s)\left[mr^2 + (m_s-1)\,\Omega\right]^{m+m_s}}, \tag{5}$$

which is valid for $m_s > 1$, while $B(\cdot,\cdot)$ denotes the beta function [51, eq. (8.384.1)]. The form of the PDF in (5) is functionally equivalent to the $\mathcal{F}$ distribution.[2] In terms of its physical interpretation, m denotes the fading severity whereas m_s controls the amount of shadowing of the rms signal power. Moreover, $\Omega = \mathbb{E}[r^2]$ represents the mean power. As $m_s \to 0$, the scattered signal component undergoes heavy shadowing. In contrast, as $m_s \to \infty$, there exists no shadowing in the wireless channel and therefore it corresponds to a standard Nakagami-m fading channel. Furthermore, as $m \to \infty$ and $m_s \to \infty$, the $\mathcal{F}$ composite fading model becomes increasingly deterministic, i.e., it becomes equivalent to an additive white Gaussian noise (AWGN) channel.

Based on (5), the PDF of the instantaneous SNR, γ, in an $\mathcal{F}$ composite fading channel can be straightforwardly deduced by using the variable transformation $\gamma = \overline{\gamma} r^2/\Omega$, such that

$$f_\gamma(\gamma) = \frac{m^m (m_s-1)^{m_s}\,\overline{\gamma}^{m_s}\,\gamma^{m-1}}{B(m,m_s)\left[m\gamma + (m_s-1)\,\overline{\gamma}\right]^{m+m_s}}, \tag{6}$$

where $\overline{\gamma} = \mathbb{E}[\gamma]$ denotes the corresponding average SNR. To this effect, the redefined moments,

$$\mathbb{E}[\gamma^n] \triangleq \int_0^\infty \gamma^n f_\gamma(\gamma)\,d\gamma \tag{7}$$

whereas the moment-generating function (MGF),

$$M_\gamma(s) \triangleq \int_0^\infty \exp(-s\gamma) f_\gamma(\gamma)\,d\gamma \tag{8}$$

are expressed as [52]

$$\mathbb{E}[\gamma^n] = \frac{(m_s-1)^n \overline{\gamma}^n \Gamma(m+n)\Gamma(m_s-n)}{m^n \Gamma(m)\Gamma(m_s)} \tag{9}$$

and

$$\begin{aligned} M_\gamma(-s) = {}& {}_1F_1\left(m;\,1-m_s;\,\frac{s\overline{\gamma}(m_s-1)}{m}\right) \\ &+ \frac{\Gamma(-m_s)\,s^{m_s}\overline{\gamma}^{m_s}(m_s-1)^{m_s}}{B(m,m_s)\,m^{m_s}} \\ &\times {}_1F_1\left(m+m_s;\,1+m_s;\,\frac{s\overline{\gamma}(m_s-1)}{m}\right) \end{aligned} \tag{10}$$

respectively, with ${}_1F_1(\cdot,\cdot,\cdot)$ denoting the Kummer confluent hypergeometric function [51, eq. (9.210.1)]. Similarly, with the aid of [51, eq. (3.194.1)] the envelope cumulative distribution function (CDF) is expressed as

$$\begin{aligned} F_R(r) = {}& \frac{m^{m-1} r^{2m}}{B(m,m_s)(m_s-1)^m \Omega^m} \\ &\times {}_2F_1\left(m, m+m_s, m+1; -\frac{mr^2}{(m_s-1)\Omega}\right), \end{aligned} \tag{11}$$

where ${}_2F_1(\cdot,\cdot;\cdot;\cdot)$ is the Gauss hypergeometric function [51, eq. (9.111)], whereas its respective SNR CDF is readily given by

$$\begin{aligned} F_\gamma(\gamma) = {}& \frac{m^{m-1}\gamma^m}{B(m,m_s)(m_s-1)^m \overline{\gamma}^m} \\ &\times {}_2F_1\left(m, m+m_s, m+1; -\frac{m\gamma}{(m_s-1)\overline{\gamma}}\right). \end{aligned} \tag{12}$$

It is noted that the above CDF expressions are valid for arbitrary values of the fading parameters m and m_s. However, an additional expression can be derived for the special case of arbitrary values of m_s and integer values of m.

Lemma 1: For $\gamma, \overline{\gamma} \in \mathbb{R}^+$, $m \in \mathbb{N}$ and $m_s > 1$, the outage probability under $\mathcal{F}$ composite fading conditions can be expressed as

$$\begin{aligned} F_\gamma(\gamma) = {}& \sum_{l=0}^{m-1} \binom{m-1}{l} \frac{(-1)^l}{B(m,m_s)} \left\{ \frac{1}{m_s+l} \right. \\ &\left. - \frac{(m_s-1)^{m_s+l}\,\overline{\gamma}^{m_s+l}}{(m_s+l)(m\gamma + (m_s-1)\overline{\gamma})^{m_s+l}} \right\}, \end{aligned} \tag{13}$$

where $\binom{\cdot}{\cdot}$ denotes the binomial coefficient [51, eq. (1.111)].

Proof: It is recalled that the CDF of the $\mathcal{F}$ composite statistical distribution is given by

$$F_\gamma(\gamma) = \int_0^\gamma \frac{m^m (m_s-1)^{m_s}\,\overline{\gamma}^{m_s} x^{m-1}}{B(m,m_s)\left[mx + (m_s-1)\,\overline{\gamma}\right]^{m+m_s}} dx. \tag{14}$$

[1] It is worth highlighting that in the present paper, we have modified slightly the underlying inverse Nakagami-m PDF from that used in [49] and subsequently the PDF for the $\mathcal{F}$ composite fading model. While the PDF in [49] is completely valid for physical channel characterization, it has some limitations in its admissible parameter range when used in analyses relating to digital communications. The redefined PDF in (5), on the other hand, is well consolidated.

[2] Letting $r^2 = x, m = d_1/2, m_s = d_2/2, \Omega = d_2/(d_2-2)$ and performing the required transformation yields the $\mathcal{F}$ distribution, $f_X(x)$, with parameters d_1 and d_2.

By setting

$$u = mx + (m_s - 1)\overline{\gamma} \tag{15}$$

and after some algebraic manipulations, it follows that

$$F_\gamma(\gamma) = \frac{(m_s-1)^{m_s}\overline{\gamma}^{m_s}}{B(m, m_s)} \times \int_{(m_s-1)\overline{\gamma}}^{m\gamma+(m_s-1)\overline{\gamma}} \frac{(u-(m_s-1)\overline{\gamma})^{m-1}}{u^{m+m_s}} du. \tag{16}$$

By applying the binomial theorem in [51, eq. (1.111)], one obtains

$$F_\gamma(\gamma) = \frac{(m_s-1)^{m_s}\overline{\gamma}^{m_s}}{B(m, m_s)} \sum_{l=0}^{m-1} \binom{m-1}{l} (1-m_s)^l \overline{\gamma}^l \times \int_{(m_s-1)\overline{\gamma}}^{m\gamma+(m_s-1)\overline{\gamma}} \frac{1}{u^{m_s+l+1}} du \tag{17}$$

which is valid when $m \in \mathbb{N}$. Consequently, the above integral can be evaluated straightforwardly. Based on this and after some algebraic manipulations, the simplified expression for the CDF in (13) is deduced, which completes the proof. □

The derived expression in Lemma 1 is novel and has a relatively simple algebraic representation. Therefore, it is useful in cumbersome analyses relating to digital communications over $\mathcal{F}$ composite fading channels, where (13) proves intractable to lead to the derivation of useful analytic solutions.

In the sequel, we use these results for the $\mathcal{F}$ composite model to perform a comprehensive capacity analysis for the cases of receiver CSI and transmitter/receiver CSI.

III. CHANNEL CAPACITY WITH RECEIVER CSI

Channel capacity is a core performance metric in conventional and emerging communication systems, and its limits are largely affected by the incurred fading conditions during wireless transmission. Ergodic capacity is the most widely used capacity measure and is concerned with CSI knowledge only at the receiver and a fixed transmit power. The effective capacity is also a particularly useful information theoretic measure as it accounts for the achievable capacity subject to the incurred latency relating to the corresponding buffer occupancy. In what follows, we derive novel exact, approximate and asymptotic analytic expressions for these two measures, namely C_{ORA} and C_{eff}, over $\mathcal{F}$ composite fading conditions.

A. ERGODIC CAPACITY

A closed-form expression for the ergodic capacity is derived in the following theorem.

Theorem 1: For $m, \gamma, \overline{\gamma}, B \in \mathbb{R}^+$ and $m_s > 1$, the channel capacity per unit bandwidth with optimum rate adaptation under $\mathcal{F}$ composite fading conditions can be expressed as

$$\frac{C_{ORA}}{B} = \frac{\psi(m+m_s)-\psi(m_s)}{\ln(2)} + \frac{(m_s-1)\overline{\gamma}-m}{(m+m_s)\ln(2)} {}_3F_2\left(1, 1, 1+m; 2, 1+m+m_s; \mathcal{D}_1\right), \tag{18}$$

where

$$\mathcal{D}_1 = \frac{m-(m_s-1)\overline{\gamma}}{m} \tag{19}$$

whereas B denotes the channel bandwidth, $\psi(\cdot)$ is the digamma function, $\ln(\cdot)$ is the natural logarithm and ${}_3F_2(\cdot,\cdot,\cdot;\cdot,\cdot;\cdot)$ is a special case of the generalized hypergeometric function ${}_pF_q(\cdot,\cdot,...,\cdot;\cdot,...,\cdot;\cdot)$, with $p = 3$ and $q = 2$ [51].

Proof: It is recalled that the channel capacity with optimum rate adaptation in the presence of fading is defined as

$$C_{ORA} \triangleq B \int_0^\infty \log_2(1+\gamma) f_\gamma(\gamma) d\gamma. \tag{20}$$

Therefore, by substituting (6) in (20), the C_{ORA} per unit bandwidth for the case of $\mathcal{F}$ composite fading channels is given by

$$\frac{C_{ORA}}{B} = \frac{m^m (m_s-1)^{m_s}\overline{\gamma}^{m_s}}{B(m, m_s)} \times \int_0^\infty \frac{\gamma^{m-1}\log_2(1+\gamma)}{[m\gamma+(m_s-1)\overline{\gamma}]^{m+m_s}} d\gamma. \tag{21}$$

The involved integral in (21) can be expressed in closed-form using [53, eq. (2.6.2.7)] as well as the logarithmic and hypergeometric function identities [51], [53]. By performing the necessary change of variables and after some algebraic manipulations, (18) is deduced, which completes the proof.

It is worth highlighting that (18) is expressed in terms of widely known functions, which are readily available in most standard scientific software packages. Nonetheless, an accurate closed-form approximation can be also deduced as a special case.

Proposition 1: For $m, \gamma, \overline{\gamma}, B \in \mathbb{R}^+$, $m_s > 1$ and $m_s \gg m$, the channel capacity per unit bandwidth with optimum rate adaptation over $\mathcal{F}$ composite fading channels can be tightly approximated as follows:

$$\frac{C_{ORA}^{appr.}}{B} \approx \frac{1}{\ln(2)} \frac{(m_s-1)\overline{\gamma}-m}{m_s} \times {}_3F_2\left(1, 1, 1+m; 2, 1+m+m_s; \mathcal{D}_1\right). \tag{22}$$

Proof: It is obvious that

$$m + m_s \approx m_s \tag{23}$$

when $m_s \gg m$. By recalling (18) and the properties of the digamma function [51], [53], it is evident that

$$\psi(m+m_s) \approx \psi(m_s) \tag{24}$$

when $m_s \gg m$, which yields

$$\psi(m+m_s) - \psi(m_s) \longrightarrow 0. \tag{25}$$

Based on the above, (18) reduces to (22), which completes the proof. □

In the same context, a particularly simple and tight asymptotic expression is derived for the case of high average SNR values.

Proposition 2: For $m, \gamma, \overline{\gamma}, B \in \mathbb{R}^+$, $m_s > 1$ and $\overline{\gamma} \gg 0$, the channel capacity per unit bandwidth with optimum rate adaptation over $\mathcal{F}$ composite fading channels can be asymptotically expressed as follows:

$$\frac{C_{ORA}^{asym.}}{B} \simeq \frac{\ln(\overline{\gamma}) + \ln(m_s - 1) - \ln(m) + \psi(m) - \psi(m_s)}{\ln(2)}. \tag{26}$$

Proof: The ergodic capacity per unit bandwidth at the high SNR regime can be accurately expressed as [54], [55]

$$C_{ORA}(\overline{\gamma}) \simeq \frac{\ln(\overline{\gamma})}{\ln(2)} + \frac{1}{\ln(2)} \frac{\partial}{\partial n} AF_{\overline{\gamma}}^{(n)}\Big|_{n=0} \tag{27}$$

$$= \frac{1}{\ln(2)} \frac{\partial}{\partial n} \mathbb{E}[\gamma^n]\Big|_{n=0} \tag{28}$$

where

$$AF \triangleq \frac{\mathbb{E}[\gamma^n]}{\mathbb{E}[\gamma]^n} - 1 \tag{29}$$

denotes the corresponding amount of fading. It is recalled that the moments of the $\mathcal{F}$ composite fading model are given in (9); therefore, the asymptotic capacity for this case can be derived by determining the first derivative of (9) with respect to n and then setting $n = 0$, namely

$$C_{ORA}^{asym.} = \frac{\partial}{\partial n} \left[\frac{(m_s - 1)^n \overline{\gamma}^n \Gamma(m+n)\Gamma(m_s - n)}{\ln(2) m^n \Gamma(m)\Gamma(m_s)} \right]_{n=0}. \tag{30}$$

Following from this, with the aid of the properties of the gamma function along with some algebraic manipulations, the first derivative of (9) for the case of the $\mathcal{F}$ composite fading with respect to n is expressed by the following closed-form representation

$$\frac{\partial}{\partial n} \mathbb{E}[\gamma^n] = \frac{(m_s - 1)^n \overline{\gamma}^n \Gamma(m+n)\Gamma(m_s - n)}{m^n B(m, m_s)\Gamma(m + m_s)} \times \left\{ \psi(m+n) - \psi(m_s - n) - \ln\left(\frac{m}{(m_s - 1)\overline{\gamma}} \right) \right\}. \tag{31}$$

By substituting (31) in (30), setting $n = 0$, i.e. $(1/\ln(2))\partial \mathbb{E}[\gamma^n]/\partial n|_{n=0}$, and carrying out some algebraic manipulations, (26) is deduced, which completes the proof. □

It is noted that the simple algebraic representation of (26) provides useful insights on the impact of the involved parameters on the overall system performance. This is also evident through the fact that it can be also expressed in terms of $\overline{\gamma}$, namely

$$\overline{\gamma}_{ORA} \approx 2^{\frac{C_{ORA}^{asym.}}{B}} e^{\psi(m_s) - \psi(m)} \frac{m}{m_s - 1}, \tag{32}$$

which provides insights on the value of $\overline{\gamma}_{ORA}$ for fixed C_{ORA}, B and fading parameters. Hence, this is useful in quantifying the required average SNR value for meeting target quality of service and bandwidth requirements under different fading conditions.

B. EFFECTIVE CAPACITY

It is recalled that the effective rate accounts for the channel capacity as a function of the asymptotic decay rate of the corresponding buffer occupancy. This is an insightful measure, particularly in emerging technologies where latency is a critical quality of service criterion.

Theorem 2: For $m, \gamma, \overline{\gamma}, \theta, B, T \in \mathbb{R}^+$ and $m_s > 1$, the effective capacity $C_{eff} = E_c(\theta)$ under $\mathcal{F}$ composite fading conditions can be expressed as

$$C_{eff} = \frac{m_s}{A} \log_2\left(\frac{m}{(m_s - 1)\overline{\gamma}} \right) + \frac{1}{A} \log_2\left(\frac{(m + m_s)_A}{(m_s)_A} \right) - \frac{\log_2\left({}_2F_1\left(A + m_s, m + m_s; A + m + m_s; \mathcal{D}_1 \right) \right)}{A}, \tag{33}$$

where

$$(x)_n \triangleq \frac{\Gamma(x+n)}{\Gamma(x)} \tag{34}$$

denotes the Pochhammer symbol [51] and

$$A = \frac{BT\theta}{\ln(2)} \tag{35}$$

is a metric of delay constraint with B and T denoting the system bandwidth and the block/frame length, respectively, whereas θ represents the quality of service (QoS) exponent in terms of the corresponding asymptotic decay rate of the buffer occupancy.

Proof: Given the instantaneous service rate of a system as

$$R = TB \log_2(1 + \gamma) \tag{36}$$

the corresponding effective rate can be expressed as

$$E_c(\theta) = -A^{-1} \log_2\left(\mathbb{E}\left[e^{-\theta R} \right] \right), \tag{37}$$

which can be re-written as [43], [56], [57]

$$C_{eff} = -\frac{1}{A} \log_2\left(\int_0^\infty e^{-\theta TB \log_2(1+\gamma)} f_\gamma(\gamma) d\gamma \right), \tag{38}$$

where $f_\gamma(\gamma)$ accounts for the corresponding fading statistics. Therefore, for the case of $\mathcal{F}$ composite fading channels, we substitute the redefined PDF in (6) into (38), which after some algebraic manipulations yields

$$C_{eff} = \frac{1}{A} \log_2\left(\frac{B(m, m_s)}{m^m (m_s - 1)^{m_s} \overline{\gamma}^{m_s}} \right) - \frac{1}{A} \log_2\left(\int_0^\infty \frac{\gamma^{m-1} d\gamma}{(1+\gamma)^A [m\gamma + (m_s - 1)\overline{\gamma}]^{m+m_s}} \right). \tag{39}$$

The integral in (39) can be expressed in closed-form with the aid of [51, eq. (3.259.3)]. Therefore, by performing the necessary change of variables one obtains the following closed-form expression

$$C_{eff} = -\frac{1}{A} \log_2\left\{ \frac{B(m, A + m_s)}{B(m, m_s)} \left(\frac{(m_s - 1)\overline{\gamma}}{m} \right)^{m_s} \times {}_2F_1\left(A + m_s, m + m_s; A + m + m_s; \mathcal{D}_1 \right) \right\}. \tag{40}$$

To this effect and by also applying the properties and identities of the logarithm, gamma and beta functions, (40) reduces to the compact form of (33), which completes the proof. □

It is noted that similar expressions to (33) were derived in [47] and [48]. However, these expressions are limited due to the constrained consideration of the SNR PDF of the $\mathcal{F}$ fading model in [49]. As a result, the derived result in Theorem 2 is more suitable since it is based on the well consolidated SNR PDF in (6). Furthermore, the corresponding analytic expression in [48] can be readily modified in order to lead to more generic, and practically more useful and reliable results. In addition, this expression can be used as a benchmark for the derivation of simple tight bounds and an accurate approximation, which provide useful insights on the impact of the involved parameters on the system performance.

Proposition 3: For $m, \gamma, \overline{\gamma}, \theta, B, T \in \mathbb{R}^+$, $m_s > 1$ *and assuming* $m_s + m \gg A$ *and* $\overline{\gamma} \geq 10dB$, *the effective capacity under* $\mathcal{F}$ *composite fading conditions can be bounded by the following inequalities*[3]*:*

$$C_{eff}^{UB} < \frac{\log_2\left((m_s+A)_m\right) - \log_2\left((m_s)_m\right)}{A} + \log_2\left(\overline{\gamma}\right) + \log_2\left(m_s - 1\right) - \log_2\left(m\right) \quad (41)$$

and

$$C_{eff}^{LB} > \log_2\left(\overline{\gamma}\right) + \log_2\left(\frac{m_s-1}{m}\right) - \frac{\log_2\left((m_s)_A\right)}{A}, \quad (42)$$

which constitute tight upper and lower bounds, respectively, to (33).

Proof: It is evident that

$$A + m + m_s \approx m + m_s \quad (43)$$

when $m + m_s \gg A$. As a result, (33) can be tightly upper bounded as follows:

$$C_{eff}^{UB} < -\frac{1}{A}\log_2\left\{\frac{(m_s)_A}{(m_s+m)_A}\left(\frac{(m_s-1)\overline{\gamma}}{m}\right)^{m_s} \times {}_2F_1\left(A+m_s, m+m_s; m+m_s; \mathcal{D}_1\right)\right\}. \quad (44)$$

Given that

$${}_2F_1\left(A+m_s, m+m_s; m+m_s; \mathcal{D}_1\right) = {}_1F_0\left(A+m_s; ; \mathcal{D}_1\right) \quad (45)$$

and by recalling that

$${}_1F_0(n; ; 1+x) \triangleq \frac{(-1)^n}{x^n} \quad (46)$$

when $n \in \mathbb{R}$, (44) reduces to

$$C_{eff}^{UB} < -\frac{1}{A}\log_2\left(\frac{(m_s)_A (m_s-1)^{m_s}\overline{\gamma}^{m_s}}{(m_s+m)_A m^{m_s}}\left(\frac{m}{(m_s-1)\overline{\gamma}}\right)^{A+m_s}\right). \quad (47)$$

To this effect and after some algebraic manipulations, the closed-form upper bound in (41) is deduced.

[3]It is noted that $(m_s+m)_A/(m_s)_A = (m_s+A)_m/(m_s)_m = \Gamma(m_s+m+A)\Gamma(m_s)/(\Gamma(m_s+m)\Gamma(m_s+A))$.

Based on (41) and recalling that $A+m+m_s \approx m+m_s$ when $m + m_s \gg A$, the left hand side term on the fraction of (41) can be reasonably eliminated. This readily yields (42), which is a tight lower bound to the exact effective capacity in (33) for the given conditions and thus, it completes the proof. □

It is noted here that (41) and (42) are particularly insightful and they can be also expressed in terms of the involved average SNR, namely

$$\overline{\gamma}_{eff} \simeq \frac{m 2^{C_{eff}^{UB}}}{m_s - 1}\left(\frac{(m_s)_A}{(m_s+m)_A}\right)^{\frac{1}{A}} \simeq \frac{m 2^{C_{eff}^{LB}}}{m_s - 1}\left((m_s)_A\right)^{\frac{1}{A}}, \quad (48)$$

which is rather accurate when $m + m_s \gg A$. Importantly, this allows the determination of $\overline{\gamma}$ for different values of m, m_s and A along with specific values of C_{eff}. This is useful in determining the required SNR for specific fading conditions and target quality of service requirements, particularly in emerging wireless communication systems.

In the same context as with the derived bounds in Proposition 3, a simple and accurate approximate expression to (33) can be additionally derived.

Proposition 4: For $m, \gamma, \overline{\gamma}, B \in \mathbb{R}^+$, $m_s > 1$ *and* $\overline{\gamma} \gg 0$, *the effective capacity under* $\mathcal{F}$ *composite fading conditions can be accurately approximated as follows:*

$$C_{eff}^{appr.} \simeq -\frac{1}{A}\log_2\left({}_2F_1(A, m_s; A+m+m_s; 1-\overline{\gamma})\right). \quad (49)$$

Proof: In the high SNR regime, i.e. $\overline{\gamma} \gg 0$, it readily follows that $\overline{\gamma} \gg m$, $\overline{\gamma} \gg m_s$ and $\overline{\gamma} \gg A$. To this effect and by expanding the logarithmic terms in (33), one obtains

$$\frac{(m_s)_A}{(m+m_s)_A}\left(\frac{(m_s-1)\overline{\gamma}}{m}\right)^{m_s} \simeq \overline{\gamma}^{m_s}. \quad (50)$$

Based on this and after some algebraic manipulations, (49) is deduced, which completes the proof. □

It is evident that (49) can be also solved with respect to the average SNR, namely

$$\overline{\gamma}_{eff} \simeq 1 - {}_2F_1^{-1}\left(A, m_s; A+m+m_s; 2^{-AC_{eff}^{appr.}}\right), \quad (51)$$

where ${}_2F_1^{-1}(\cdot,\cdot;\cdot;\cdot)$ denotes the inverse Gauss hypergeometric function.

To the best of the authors knowledge, the analytic expressions provided here have not been previously reported in the open technical literature.

IV. CHANNEL CAPACITY WITH TRANSMITTER AND RECEIVER CSI

The previous section was devoted to the capacity analysis for the case of known CSI at the receiver side. However, in several emerging systems, CSI can be also available at the transmitter as this allows greater flexibility and adaptability, which results in a more efficient and intelligent overall system operation. A typical feature in the case of knowing CSI at the transmitter and at the receiver is the ability to benefit from adaptive transmit power. This is the key process of the so called water-filling approach and in fixed rate systems. In the former, higher power and rate levels are allocated in

good fading conditions and less power in severe fading conditions. In the latter, the transmitter adapts the power accordingly in order to maintain a fixed rate at the receiver [52]. These concepts are critical in numerous emerging applications that are characterized by stringent quality of service requirements, such as telemedicine and vehicle to vehicle communications [49]. Subsequently, this section is devoted to the capacity analysis over $\mathcal{F}$ composite fading channels for the following adaptation policies: i) optimum power and rate adaptation; ii) channel inversion with fixed rate; iii) truncated channel inversion with fixed rate.

A. OPTIMUM POWER AND RATE ADAPTATION

This policy is based on the aforementioned water-filling concept and it is characterized by a power constraint, which ensures a more efficient operation [52].

Theorem 3: For $m, \gamma, \overline{\gamma}, B, \gamma_0 \in \mathbb{R}^+$, and $m_s > 1$, the channel capacity per unit bandwidth with optimum power and rate adaptation under $\mathcal{F}$ composite fading conditions can be expressed as

$$\frac{C_{OPRA}}{B} = \frac{(m_s-1)^{m_s}\overline{\gamma}^{m_s}}{\ln(2)B(m,m_s)m_s^2\, m^{m_s}\gamma_0^{m_s}} \times {}_3F_2\left(m_s, m_s, m+m_s; 1+m_s, 1+m_s; \mathcal{D}_2\right), \quad (52)$$

where

$$\mathcal{D}_2 = \frac{(1-m_s)\overline{\gamma}}{m\gamma_0} \quad (53)$$

with γ_0 denoting the SNR threshold that determines transmission.

Proof: It is recalled that the channel capacity with optimum power and rate adaptation over fading channels is defined as [5], [6], [52]

$$C_{OPRA} = B\int_{\gamma_0}^{\infty} \log_2\left(\frac{\gamma}{\gamma_0}\right) f_\gamma(\gamma)d\gamma. \quad (54)$$

Therefore, for the case of $\mathcal{F}$ composite fading channels, we substitute (6) in (54), which yields

$$\frac{C_{OPRA}}{B} = \frac{m^m(m_s-1)^{m_s}\,\overline{\gamma}^{m_s}}{B(m,m_s)\ln(2)} \times \int_{\gamma_0}^{\infty} \frac{\ln(\gamma/\gamma_0)\gamma^{m-1}}{(m\gamma+(m_s-1)\overline{\gamma})^{m+m_s}}d\gamma. \quad (55)$$

The integral in (55) can be expressed in closed-form with the aid of [53]. To this effect, by performing the necessary variable transformation, utilizing the hypergeometric function identities in [51] and [53] and carrying out some algebraic manipulations, one obtains (52), which completes the proof. □

Remark 1: It is noted that the C_{OPRA} in Theorem 3 can be alternatively expressed equivalently as follows:

$$\frac{C_{OPRA}}{B} = \frac{\ln(\overline{\gamma})+\ln(m_s-1)-\ln(m)+\psi(m)-\psi(m_s)}{\ln(2)} + \frac{m^{m-2}\gamma_0^m}{\ln(2)(m_s-1)^m\,\overline{\gamma}^m B(m,m_s)} \times {}_3F_2\left(m, m, m+m_s; 1+m, 1+m; \frac{m\gamma_0}{(1-m_s)\,\overline{\gamma}}\right) - \frac{m^{m-1}\gamma_0^m\ln(\gamma_0)}{\ln(2)(m_s-1)^m\,\overline{\gamma}^m B(m,m_s)} \times {}_2F_1\left(m, m+m_s; 1+m; \frac{m\gamma_0}{(1-m_s)\,\overline{\gamma}}\right) - \frac{\ln(\gamma_0)(m_s-1)^{m_s}\,\overline{\gamma}^{m_s}}{\ln(2)m_s m^{m_s}\gamma_0^{m_s}B(m,m_s)} \times {}_2F_1\left(m_s, m+m_s; 1+m_s; \frac{(1-m_s)\,\overline{\gamma}}{m\gamma_0}\right). \quad (56)$$

It is worth noting that (52) is tractable both analytically and numerically. Likewise, (56) has the same algebraic representation as (52) but it is less suitable because it involves more terms. Nonetheless, (56) can be useful in that it can be used as a benchmark for the derivation of an accurate approximation for the considered scenario, which is both simple and insightful.

Proposition 5: For $m, \gamma, \gamma_0, B \in \mathbb{R}^+$, $m_s > 1$ and $\overline{\gamma} \gg 0$, the channel capacity per unit bandwidth with optimum power and rate adaptation under $\mathcal{F}$ composite fading conditions can be accurately approximated by the following closed-form representation

$$\frac{C_{OPRA}^{appr.}}{B} \approx \log_2(\overline{\gamma}) - \log_2(\gamma_0)(m_s-1)^{m_s}\,\overline{\gamma}^{m_s}\mathcal{D}_3, \quad (57)$$

where

$$\mathcal{D}_3 = {}_2F_1\left(m_s, m+m_s; 1+m_s; \frac{(1-m_s)\,\overline{\gamma}}{m\gamma_0}\right). \quad (58)$$

Proof: It is evident that at the high average SNR regime, the argument of the first two hypergeometric function in (52) tends to zero i.e.

$$\frac{m\gamma_0}{(1-m_s)\overline{\gamma}} \longrightarrow 0. \quad (59)$$

To this effect and by recalling the hypergeomeric function property

$${}_pF_q(a_1, a_2, \cdots; b_1, b_2, \cdots; 0) \triangleq 1 \quad (60)$$

it immediately follows that

$$\frac{C_{OPRA}^{appr.}}{B} \approx \frac{\ln(m_s-1)+\ln(\overline{\gamma})+\psi(m)-\psi(m_s)-\ln(m)}{\ln(2)} + \frac{m^{m-2}\gamma_0^m - m^{m-1}\gamma_0^m\ln(\gamma_0)}{\ln(2)\overline{\gamma}^m(m_s-1)^m B(m,m_s)} - \frac{\ln(\gamma_0)\overline{\gamma}^{m_s}(m_s-1)^{m_s}}{\ln(2)m_s m^{m_s}\gamma_0^{m_s}B(m,m_s)} \times {}_2F_1\left(m_s, m+m_s; 1+m_s; \frac{\overline{\gamma}(1-m_s)}{m\gamma_0}\right). \quad (61)$$

Given also the practical range of values of γ_0, [5]–[7], [52], it is reasonable to assume that

$$m^{m-2} \simeq m^{m-1}\ln(\gamma_0), \quad (62)$$

which yields

$$\frac{C_{OPRA}^{appr.}}{B} \approx \frac{\ln(m_s-1)+\ln(\overline{\gamma})+\psi(m)-\psi(m_s)-\ln(m)}{\ln(2)} - \frac{\ln(\gamma_0)\overline{\gamma}^{m_s}(m_s-1)^{m_s}}{\ln(2)m_s m^{m_s}\gamma_0^{m_s}B(m,m_s)} \times {}_2F_1\left(m_s, m+m_s; 1+m_s; \frac{\overline{\gamma}(1-m_s)}{m\gamma_0}\right). \tag{63}$$

It is evident that $\ln(\overline{\gamma})$ is the dominant term of the first fraction of (63). Based on this and after some algebraic manipulations, (57) is deduced, which completes the proof. □

It is recalled that the cut-off SNR, γ_0, determines the optimum operation in this policy since when the average SNR value drops below its level, transmission is suspended. In what follows, we derive a useful analytic expression for γ_0.

Lemma 2: For $m, \gamma, \overline{\gamma}, B, \gamma_0 \in \mathbb{R}^+$, and $m_s > 1$, the optimum SNR cut-off level for the case of $\mathcal{F}$ composite fading channels can be expressed as

$$\gamma_0 = \frac{(1-m_s)\,\overline{\gamma}\,m^{-1}}{B^{-1}\left(\frac{(-1)^{m_s}(m_s-1)\overline{\gamma}B(m,m_s)}{m}; 1+m_s, 1-m-m_s\right)}, \tag{64}$$

where $B^{-1}(\cdot;\cdot,\cdot)$ denotes the inverse incomplete beta function.

Proof: It is recalled that the optimum cut off SNR in the case of optimum power and rate adaptation must satisfy the following expression

$$\int_{\gamma_0}^{\infty}\left(\frac{1}{\gamma_0}-\frac{1}{\gamma}\right)f_\gamma(\gamma)d\gamma = 1, \tag{65}$$

which yields

$$\gamma_0 = \int_{\gamma_0}^{\infty} f_\gamma(\gamma)d\gamma - \gamma_0\int_{\gamma_0}^{\infty}\frac{f_\gamma(\gamma)}{\gamma}d\gamma. \tag{66}$$

By substituting (6) in (66), we obtain (67) at the top of the next page.

Then, by taking the first derivative in both sides of (67) and carrying out some algebraic manipulations, one obtains

$$\int_{\gamma_0}^{\infty}\frac{m^m(m_s-1)^{m_s}\,\overline{\gamma}^{m_s}\gamma^{m-2}}{B\,(m,m_s)\,[m\gamma+(m_s-1)\,\overline{\gamma}\,]^{m+m_s}}d\gamma = -1. \tag{68}$$

The above integral can be expressed in closed-form with the aid of the incomplete beta function in [51, eq. (8.391)], which yields

$$B\left(\frac{(1-m_s)\overline{\gamma}}{m\gamma_0}; 1+m_s, 1-m-m_s\right)\mathcal{D}_2 = -1, \tag{69}$$

where

$$\mathcal{D}_2 = \frac{m(-1)^{-1-m_s}}{B(m,m_s)(m_s-1)\,\overline{\gamma}}. \tag{70}$$

Finally, by solving (69) with respect to γ_0 yields (64), which completes the proof. □

Remark 2: The integral in (68) can be equivalently expressed in closed-form in terms of the Gauss hypergeometric function with the aid of [51, eq. (3.194.1)]. Based on this and by following the same procedure as in Lemma 2 along with some algebraic manipulations, the following exact analytic expression can be also deduced

$$\gamma_0 = \frac{(-1)^{\frac{1}{m_s+1}}\,\overline{\gamma}^{\frac{m_s}{1+m_s}}(m_s-1)^{\frac{m_s}{1+m_s}}}{[B(m,m_s)]^{\frac{1}{1+m_s}}(1+m_s)^{\frac{1}{1+m_s}}m^{\frac{m_s}{1+m_s}}} \times\left[{}_2F_1\left(m_s+1, m+m_s; m_s+2; \frac{(1-m_s)\overline{\gamma}}{m\gamma_0}\right)\right]^{\frac{1}{1+m_s}}, \tag{71}$$

which can be evaluated numerically with the aid of standard mathematical software packages.

B. CHANNEL INVERSION WITH FIXED RATE

This policy ensures a fixed data rate at the receiver by means of inverting the channel and adapting the transmit power accordingly. This is particularly useful in numerous applications where a fixed rate is the core requirement. In what follows, we derive the channel capacity with channel inversion and fixed rate in the presence of $\mathcal{F}$ composite fading conditions [5]–[7], [52].

Theorem 4: For $m, \gamma, \overline{\gamma}, B \in \mathbb{R}^+$ and $m_s > 1$, the channel capacity per unit bandwidth with channel inversion and fixed rate under $\mathcal{F}$ composite fading conditions can be expressed as follows:

$$\frac{C_{CIFR}}{B} = \log_2\left(1+\frac{(m-1)(m_s-1)\,\overline{\gamma}}{m\,m_s}\right). \tag{72}$$

Proof: The channel capacity with channel inversion and fixed rate is defined as

$$C_{CIFR} = B\log_2\left(1+\frac{1}{\int_0^{\infty}\frac{f_\gamma(\gamma)}{\gamma}d\gamma}\right). \tag{73}$$

Therefore, for the case of $\mathcal{F}$ composite fading conditions, we substitute (6) into (72), yielding

$$\frac{C_{CIFR}}{B} = \log_2\left(1+\frac{B(m,m_s)m^{-m}(m_s-1)^{-m_s}\overline{\gamma}^{-m_s}}{\int_0^{\infty}\frac{\gamma^{m-1}}{[m\gamma+(m_s-1)\,\overline{\gamma}\,]^{m+m_s}}d\gamma}\right). \tag{74}$$

The above integral can be obtained in closed-form using [51, eq. (3.194.3)]. To this end, by making the necessary change of variables and substituting in (74) one obtains

$$\frac{C_{CIFR}}{B} = \log_2\left(1+\frac{B(m,m_s)\Gamma(m+m_s)(m_s-1)\,\overline{\gamma}}{m\Gamma(m-1)\Gamma(m_s+1)}\right), \tag{75}$$

which with the aid of the properties of the beta and gamma functions and after some algebraic manipulations yields (72), which completes the proof. □

$$\int_{\gamma_0}^{\infty} \frac{m^m (m_s-1)^{m_s}\,\overline{\gamma}^{m_s}\gamma^{m-1}}{B\,(m,m_s)\,[m\gamma+(m_s-1)\,\overline{\gamma}\,]^{m+m_s}}d\gamma = \gamma_0 + \gamma_0 \int_{\gamma_0}^{\infty} \frac{m^m (m_s-1)^{m_s}\,\overline{\gamma}^{m_s}\gamma^{m-2}}{B\,(m,m_s)\,[m\gamma+(m_s-1)\,\overline{\gamma}\,]^{m+m_s}}d\gamma. \tag{67}$$

It is evident that (72) has a rather simple algebraic representation. Furthermore, it is particularly insightful since it can be expressed exactly in terms of the average SNR, namely

$$\overline{\gamma} = \frac{mm_s}{(m-1)(m_s-1)}\left(2^{\frac{C_{CIFR}}{B}}-1\right) \tag{76}$$

as well as in terms of the fading parameters m and m_s, namely

$$m = \frac{(m_s-1)\overline{\gamma}}{(m_s-1)\overline{\gamma} - m_s\left(2^{\frac{C_{CIFR}}{B}}-1\right)} \tag{77}$$

and

$$m_s = \frac{(m-1)\overline{\gamma}}{(m-1)\overline{\gamma} - m\left(2^{\frac{C_{CIFR}}{B}}-1\right)} \tag{78}$$

respectively. The above expressions can provide meaningful insight on the impact of the involved parameters on the overall system performance. Also, they are useful in determining the required average SNR values for target quality of service and bandwidth requirements under different multipath fading and shadowing conditions.

C. TRUNCATED CHANNEL INVERSION WITH FIXED RATE

Channel inversion with fixed rate constitutes a low complexity and effective method to achieve fixed rate communications. However, the main drawback of this technique is the large transmit power requirements in case of deep fades. Nonetheless, this specific issue can be resolved by inverting the channel above a fixed cut-off level, namely channel truncation. In what follows, we quantify the channel capacity with truncated channel inversion and fixed rate for the case of $\mathcal{F}$ composite fading conditions.

Theorem 5: For $\gamma, \overline{\gamma}, B \in \mathbb{R}^+$, and $m_s > 1$, the channel capacity per unit bandwidth with truncated channel inversion and fixed rate under $\mathcal{F}$ composite fading conditions can be expressed as

$$\frac{C_{TIFR}}{B} = \log_2\left(1+\frac{B(m,m_s)(m_s+1)m^{m_s}\gamma_0^{m_s+1}}{(m_s-1)^{m_s}\overline{\gamma}^{m_s}\mathcal{D}_3}\right) \times\left(1-\frac{m^{m-1}\gamma_{th}^{m}\mathcal{D}_4}{B(m,m_s)(m_s-1)^m\overline{\gamma}^m}\right) \tag{79}$$

when $m \in \mathbb{R}^+$, and

$$\frac{C_{TIFR}}{B} = \log_2\left(1+\frac{B(m,m_s)}{m(m_s-1)^{m_s}\overline{\gamma}^{m_s}\mathcal{D}_5}\right) \times\left(1-\sum_{l=0}^{m-1}\binom{m-1}{l}\frac{(-1)^l}{B(m,m_s)}\frac{1-\mathcal{D}_6}{m_s+l}\right) \tag{80}$$

when $m \in \mathbb{N}$. The terms $\mathcal{D}_3$ and $\mathcal{D}_4$ in (79) are expressed as

$$\mathcal{D}_3 = {}_2F_1\left(m_s+1, m+m_s; m_s+2; \frac{(1-m_s)\overline{\gamma}}{m\gamma_0}\right) \tag{81}$$

and

$$\mathcal{D}_4 = {}_2F_1\left(m, m+m_s; 1+m; \frac{m\gamma_{th}}{(1-m_s)\overline{\gamma}}\right), \tag{82}$$

whereas the $\mathcal{D}_5$ and $\mathcal{D}_6$ terms in (80) are given by

$$\mathcal{D}_5 = \sum_{l=0}^{m-2}\binom{m-2}{l}\frac{(-1)^l(m_s+l+1)^{-1}(m_s-1)^l\overline{\gamma}^l}{(m\gamma_0+(m_s-1)\overline{\gamma})^{m_s+l+1}} \tag{83}$$

and

$$\mathcal{D}_6 = \frac{(m_s-1)^{m_s+l}\,\overline{\gamma}^{m_s+l}}{(m\gamma_{th}+(m_s-1)\overline{\gamma})^{m_s+l}}. \tag{84}$$

Proof: The channel capacity with truncated channel inversion and fixed rate is defined as

$$C_{TIFR} \triangleq B\log_2\left(1+\frac{1}{\int_{\gamma_0}^{\infty}\frac{f_\gamma(\gamma)}{\gamma}d\gamma}\right)\int_{\gamma_0}^{\infty} f_\gamma(\gamma)d\gamma, \tag{85}$$

which with the aid of (6) for the case of $\mathcal{F}$ composite fading channels and recalling that

$$\int_{\gamma_0}^{\infty} f(x)dx = 1-\int_0^{\gamma_0} f(x)dx \tag{86}$$

$$= 1 - P_{out} \tag{87}$$

is expressed as

$$\frac{C_{TIFR}}{B} = \log_2\left(1+\frac{B(m,m_s)}{\int_{\gamma_0}^{\infty}\frac{m^m(m_s-1)^{m_s}\overline{\gamma}^{m_s}\gamma^{m-2}}{[m\gamma+(m_s-1)\overline{\gamma}\,]^{m+m_s}}d\gamma}\right) \times\left(1-\mathcal{D}_7\int_0^{\gamma_0}\frac{\gamma^{m-1}}{[m\gamma+(m_s-1)\overline{\gamma}\,]^{m+m_s}}d\gamma\right), \tag{88}$$

where

$$\mathcal{D}_7 = \frac{m^m(m_s-1)^{m_s}\overline{\gamma}^{m_s}}{B(m,m_s)}. \tag{89}$$

Now, recalling that

$$P_{out} \triangleq F(\gamma_{th}) \tag{90}$$

and using (12) for the case of $m \in \mathbb{R}^+$ along with substituting in (88), it follows that

$$\frac{C_{TIFR}}{B} = \log_2\left(1+\frac{1}{\mathcal{D}_7\int_{\gamma_0}^{\infty}\frac{\gamma^{m-2}}{[m\gamma+(m_s-1)\overline{\gamma}\,]^{m+m_s}}d\gamma}\right) \times\left(1-\frac{m^{m-1}\gamma_{th}^{m}\mathcal{D}_4}{B(m,m_s)(m_s-1)^m\overline{\gamma}^m}\right). \tag{91}$$

The integral in (91) can be expressed in closed-form with the aid of [51, eq. (3.194.1)]. This is achieved by performing the

necessary variable transformation and after some algebraic manipulations, which yields (79) for the case of $m \in \mathbb{R}^+$.

Likewise, for the case of $m \in \mathbb{N}$, we apply again $P_{out} \triangleq F(\gamma_{th})$ in (13), which upon substitution in (91), it follows that

$$\frac{C_{TIFR}}{B} = \log_2\left(1 + \frac{1}{\mathcal{D}_7 \int_{\gamma_0}^{\infty} \frac{\gamma^{m-2}}{[m\gamma+(m_s-1)\overline{\gamma}\,]^{m+m_s}} d\gamma}\right) \times \left(1 - \sum_{l=0}^{m-1} \binom{m-1}{l} \frac{(-1)^l}{B(m,m_s)} \frac{1-\mathcal{D}_6}{m_s+l}\right). \quad (92)$$

Therefore, by setting

$$u = m\gamma + (m_s - 1)\overline{\gamma} \quad (93)$$

in (92), one obtains

$$\frac{C_{TIFR}}{B} = \log_2\left(1 + \frac{m^{m-1}}{\mathcal{D}_7 \int_{m\gamma_0+(m_s-1)\overline{\gamma}}^{\infty} \frac{(u-(m_s-1)\overline{\gamma})^{m-2}}{u^{m+m_s}} du}\right) \times \left(1 - \sum_{l=0}^{m-1} \binom{m-1}{l} \frac{(-1)^l}{B(m,m_s)} \frac{1-\mathcal{D}_6}{m_s+l}\right). \quad (94)$$

Now applying the binomial theorem in [51, eq. (1.111)] in the above integral along with some algebraic manipulations yields

$$\frac{C_{TIFR}}{B} = \log_2\left(1 + \frac{B(m,m_s)m^{-1}(m_s-1)^{-m_s}\overline{\gamma}^{-m_s}}{\sum_{l=0}^{m-2}\binom{m-2}{l}(-1)^l(m_s-1)^l\overline{\gamma}^{\,l}\mathcal{D}_8}\right) \times \left(1 - \sum_{l=0}^{m-1} \binom{m-1}{l} \frac{(-1)^l}{B(m,m_s)} \frac{1-\mathcal{D}_6}{m_s+l}\right), \quad (95)$$

where

$$\mathcal{D}_8 = \int_{m\gamma_0+(m_s-1)\overline{\gamma}}^{\infty} u^{-m_s-l-2} du. \quad (96)$$

It is evident that the integral above can be evaluated straightforwardly, which yields (80) and completes the proof for the case of $m \in \mathbb{N}$. □

Remark 3: It is noted that the integral in (91) *can be alternatively expressed equivalently in closed-form in terms of the incomplete beta function [51]. As a result, the channel capacity with truncated channel inversion and fixed rate over $\mathcal{F}$ composite fading channels can be additionally expressed as follows:*

$$\frac{C_{TIFR}}{B} = \log_2\left(1 + \frac{(-1)^{m_s}B(m,m_s)(1-m_s)\overline{\gamma}}{mB\left(\frac{(1-m_s)\overline{\gamma}}{m\gamma_0}; 1+m_s, 1-m-m_s\right)}\right) \times \left(1 - \frac{m^{m-1}\gamma_{th}^m\mathcal{D}_4}{B(m,m_s)(m_s-1)^m\overline{\gamma}^m}\right), \quad (97)$$

which holds for $m \in \mathbb{R}^+$.

The exact analytic expressions in Theorem 5 are tractable both analytically and numerically. However, capitalizing on them leads to the derivation of a simple lower bound which is both insightful and tight since it can be also regarded as an accurate approximation.

Proposition 6: For $\gamma, \overline{\gamma}, \gamma_0, B \in \mathbb{R}^+$, $m \in \mathbb{N}$, $m_s > 1$ and $\overline{\gamma} \gg \gamma_{th}$, the channel capacity per unit bandwidth with truncated channel inversion and fixed rate under $\mathcal{F}$ composite fading conditions can be tightly lower bounded and approximated as follows:

$$\frac{C_{TIFR}^{LB}}{B} < \log_2\left(1 + \frac{B(m,m_s)(m_s-1)\overline{\gamma}}{m\sum_{l=0}^{m-2}\binom{m-2}{l}\frac{(-1)^l}{m_s+l+1}}\right). \quad (98)$$

Proof: By recalling the case of $m \in \mathbb{N}$ in Theorem 5 and assuming large average SNR values, it follows that (80) can be accurately approximated by the simplified representation in (99), at the bottom of the next page. To this effect and by assuming that $\overline{\gamma} \gg \gamma_{th}$, (99) reduces to

$$\frac{C_{TIFR}^{LB.}}{B} \approx \log_2\left(1 + \frac{B(m,m_s)m^{-1}(m_s-1)^{-m_s}\overline{\gamma}^{-m_s}}{\sum_{l=0}^{m-2}\binom{m-2}{l}\frac{(-1)^l}{(m_s+l+1)((m_s-1)\overline{\gamma})^{m_s+1}}}\right) \quad (100)$$

which after some algebraic manipulations yields (98), which completes the proof. □

Remark 4: It is noted that (98) *is a simple lower bound to the exact analytic expression in* (80) *which is so accurate that can be also regarded as a simple and accurate closed-form approximation, i.e. $C_{TIFR}^{LB} = C_{TIFR}^{appr.}$. This approximation is also tight even for comparable values of $\overline{\gamma}$ and $\overline{\gamma}_{th}$; as a result, the use of* (98) *as an approximation is not constrained by the condition $\overline{\gamma} \gg \gamma_{th}$ in Proposition 6.*

It is also worth noting that (98) is rather insightful as it can be expressed in terms of $\overline{\gamma}$, namely

$$\overline{\gamma} \approx \frac{2^{\frac{C_{TIFR}^{appr.}}{B}} - 1}{B(m,m_s)(m_s-1)} \sum_{l=0}^{m-2} \binom{m-2}{l} \frac{(-1)^l m}{m_s+l+1}. \quad (101)$$

As in the previous scenarios, (101) is useful for target quality of service and bandwidth requirements as it quantifies the required average SNR value for different multipath fading and shadowing conditions.

V. NUMERICAL RESULTS

In this section, we utilize the analytic results obtained in the previous sections to quantify the achievable channel capacity for the case of receiver CSI, and transmitter and receiver CSI. This is realized for various communication scenarios under realistic multipath fading and shadowing conditions. The accuracy of the proposed approximate and asymptotic expressions as well as the tightness of the proposed upper and lower bounds are also extensively quantified.

Fig. 1 illustrates the C_{ORA} per unit bandwidth over $\mathcal{F}$ composite fading channels with five different combinations of the m and m_s parameters, namely heavy shadowing ($m = 50.0$, $m_s = 1.1$), severe multipath fading ($m = 0.5$, $m_s = 50.0$), intense ($m = 0.5$, $m_s = 1.1$), moderate

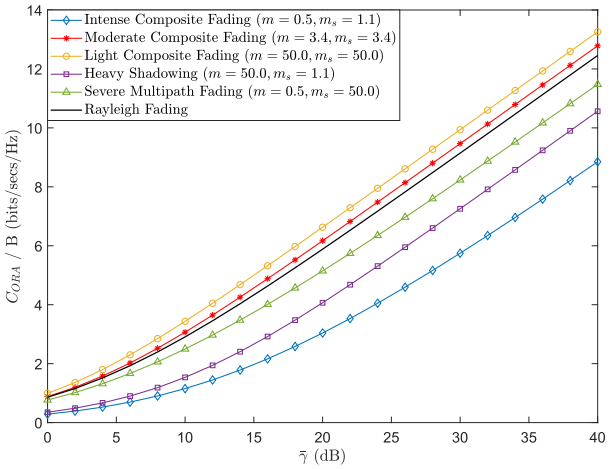

FIGURE 1. C_{ORA}/B versus average SNR under $\mathcal{F}$ fading conditions for different values of the m and m_s parameters.

TABLE 1. Exact, approximate & asymptotic C_{ORA}.

Involved Parameters			Ergodic Capacity		
m	m_s	$\overline{\gamma}$	(18)	(22)	(26)
1.2	1.2	10dB	1.76	1.40	0.73
2.2	1.2	10dB	1.87	0.91	1.06
2.2	3.2	10dB	2.96	3.11	2.67
4.8	4.8	10dB	3.19	3.11	2.98
1.2	1.2	20dB	4.27	3.92	4.06
2.2	1.2	20dB	4.52	3.56	4.39
2.2	3.2	20dB	6.03	6.17	5.99
4.8	4.8	20dB	6.33	6.25	6.31
1.2	1.2	30dB	7.41	7.05	7.38
2.2	1.2	30dB	7.72	6.76	7.71
2.2	3.2	30dB	9.31	9.46	9.31
4.8	4.8	30dB	9.63	9.55	9.63
1.2	1.2	40dB	10.71	10.35	10.70
2.2	1.2	40dB	11.03	10.07	11.03
2.2	3.2	40dB	12.63	12.78	12.63
4.8	4.8	40dB	12.95	12.87	12.95

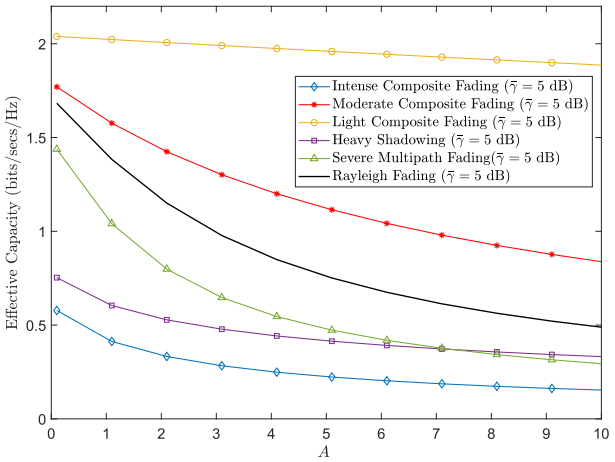

FIGURE 2. Effective capacity versus A under $\mathcal{F}$ fading channels for different values of the m and m_s parameters when $\overline{\gamma} = 5$ dB.

($m = 3.4$, $m_s = 3.4$), and light ($m = 50.0$, $m_s = 50.0$) composite fading. The C_{ORA} per unit bandwidth over Rayleigh fading channels is also illustrated in Fig. 1 for comparison. As anticipated, the lowest spectral efficiency occurs when the channel is subject to simultaneous severe multipath fading and heavy shadowing, i.e., intense composite fading. On the contrary, the highest spectral efficiency appears in the light composite fading scenarios. This is largely due to the fact that the $\mathcal{F}$ composite fading channel tends to become more deterministic, i.e., approaches an AWGN channel, as the m and m_s parameters approach infinity i.e. large m and m_s in reality. Also, the difference between the two scenarios is substantial across all SNR regimes, since the achieved channel capacity in the case of light composite fading is over 50% more than the capacity for the case of intense composite fading. Interestingly, it is noted that the spectral efficiency is higher when the channel is subject to severe multipath fading compared to the channel undergoing heavy shadowing. This suggests that the shadowing constitutes a more dominating influence on the performance of wireless communications systems, compared to the multipath fading. Furthermore, the severe multipath fading ($m = 0.5$, $m_s = 50.0$) case is equivalent to the Nakagami-m fading, for $m = 0.5$. Accordingly, as shown in Fig. 1, the Rayleigh fading case ($m = 1$) exhibits a higher spectral efficiency compared to the severe multipath fading case considered in this paper, which verifies its insufficient modeling capability.

In the same context, the accuracy of the corresponding approximate and asymptotic expressions in (22) and (26), respectively, is depicted in Table 1 against the exact analytic expression in (18). It is shown that (22) appears more accurate in low average SNR values, contrary to (26) which appears more accurate in the moderate and high SNR regimes. Nonetheless, both (22) and (26) are acceptably accurate in all multipath fading and shadowing conditions across all average SNR values, which verifies their theoretical and practical usefulness.

Fig. 2 demonstrates how the C_E per unit bandwidth varies as a function of the delay constraint over $\mathcal{F}$ composite fading channels. Five different combinations of the m and m_s parameters were considered for a case of low average SNR, i.e. $\overline{\gamma} = 5$ dB, which makes the impact of the incurred delay more critical. It is evident that the spectral efficiency is affected

$$\frac{C_{TIFR}^{appr.}}{B} \approx \log_2\left(1 + \frac{B(m, m_s)}{m(m_s-1)^{m_s}\overline{\gamma}^{m_s}\sum_{l=0}^{m-2}\binom{m-2}{l}\frac{(-1)^l(m_s-1)^l\overline{\gamma}^l}{(m_s+l+1)(m\gamma_{th}+(m_s-1)\overline{\gamma})^{m_s+l+1}}}\right). \tag{99}$$

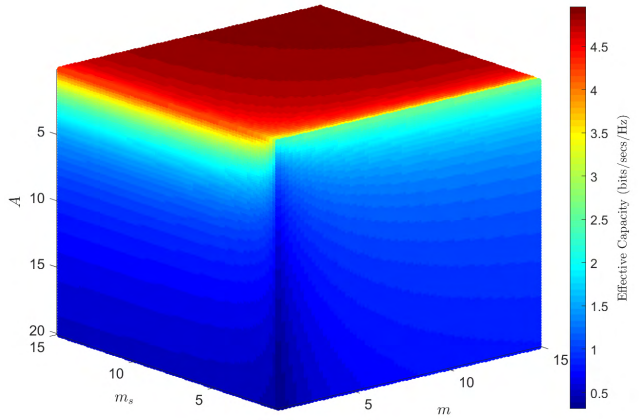

FIGURE 3. Effective capacity in an $\mathcal{F}$ fading channel as a function of the m, m_s and A parameters for $\overline{\gamma} = 15$ dB.

considerably by the value of A across all types of fading conditions, with the impact on intense fading conditions being the most detrimental. In the same context, the effects of the multipath fading and shadowing are shown in Fig. 3, where the performance of the C_E is illustrated along with different values of A and $\overline{\gamma} = 15$ dB. In all cases, we consider broad ranges of the involved parameters, namely $1 < m \leq 15$, $1 < m_s \leq 15$ and $0 \leq A \leq 20$ in order to consider all types of fading severity and incurred delays, as these are encountered in realistic communication scenarios. As expected, the spectral efficiency increases as the m and m_s parameters are greater ($m, m_s \rightarrow 15$) and A is smaller ($A \rightarrow 0$), i.e., light composite fading conditions with no delay constraint. Conversely, the performance of the C_E is rather poor for the case of intense composite fading conditions with excessive delay constraint, i.e., $m, m_s \rightarrow 1$ and $A \rightarrow 20$. In general, it is shown that even if one of the parameters is unfavorable i.e. excessive delay constraint or severe multipath fading or shadowing, the corresponding achievable C_E will lie at moderate levels, regardless of how favorable the values of the other parameters are. This verifies the need for accurate channel modeling, and latency control and reduction in the deployment of efficient wireless technologies.

Likewise, Table 2 depicts the accuracy and tightness of the proposed approximation and bounds, respectively, against the exact results. It is shown that the upper bound exhibits the most accurate behavior across all fading conditions in the low average SNR regime, and for small and moderate values of A. However, as the average SNR increases, the offered lower bound and the approximation exhibit similar accuracy. Nonetheless, as in the case of C_{ORA}, the accuracy of (41), (42) and (49) is acceptable in all fading and latency scenarios across all average SNR regimes, which verifies their usefulness.

Regarding the capacity analyses for the case of transmitter and receiver CSI, Fig. 4 demonstrates the considered C_{OPRA} per unit bandwidth for the same combinations of the m and m_s parameters used in Fig. 1, with $\gamma_0 = 1$ dB and

TABLE 2. Exact, bounded & approximate C_{eff}.

Involved Parameters				Effective Capacity			
m	m_s	$\overline{\gamma}$	A	(33)	(41)	(42)	(49)
2.5	3.0	10dB	0.4	2.80	2.82	1.56	2.37
3.2	3.0	10dB	0.4	2.87	2.97	1.21	2.23
3.2	2.3	10dB	0.4	2.73	2.76	1.02	2.02
4.5	4.5	10dB	0.4	3.09	3.12	0.82	2.34
2.5	3.0	10dB	1.0	2.57	2.62	1.42	2.19
3.2	3.0	10dB	1.0	2.66	2.77	1.06	2.07
3.2	2.3	10dB	1.0	2.51	2.54	0.82	1.83
4.5	4.5	10dB	1.0	2.92	2.96	0.79	2.22
2.5	3.0	25dB	0.4	7.43	7.59	6.52	7.13
3.2	3.0	25dB	0.4	7.53	8.56	6.19	6.97
3.2	2.3	25dB	0.4	7.34	9.58	6.00	6.64
4.5	4.5	25dB	0.4	7.81	8.33	5.87	7.12
2.5	3.0	25dB	1.0	7.04	7.06	6.37	6.85
3.2	3.0	25dB	1.0	7.20	7.99	6.04	6.69
3.2	2.3	25dB	1.0	6.97	8.81	5.80	6.27
4.5	4.5	25dB	1.0	7.59	7.94	5.77	6.95

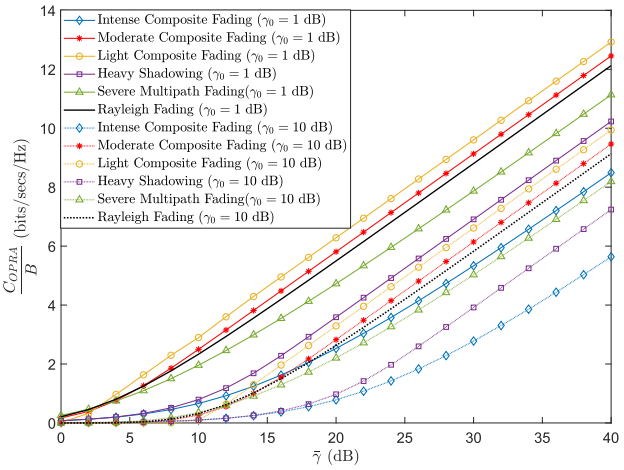

FIGURE 4. C_{OPRA}/B versus average SNR under $\mathcal{F}$ fading conditions for different values of the m and m_s parameters when $\gamma_0 = 1$ dB and $\gamma_0 = 10$ dB.

$\gamma_0 = 10$ dB. It is evident that the spectral efficiency increases as γ_0 reduces in all considered fading conditions. For example, for the case of moderate composite fading conditions at $\overline{\gamma} = 20$ dB, $C_{OPRA}/B = 5.8$ bits/secs/Hz when $\gamma_0 = 1$ dB and 2.8 bits/secs/Hz when $\gamma_0 = 10$ dB. Yet, a similar capacity trend is observed across all fading conditions for the considered γ_0 values.

Fig. 5 and Fig. 6 demonstrate the performance of the considered C_{CIFR} and C_{TIFR}, respectively, for different values of m, m_s and $\overline{\gamma}$ parameters of the $\mathcal{F}$ composite fading channels, namely $1 < m \leq 15$, $1 < m_s \leq 15$ and $0 \leq \overline{\gamma} \leq 40$ dB. It is also noted that the value of γ_0 for Fig. 6 was set to 5 dB. As expected, for both C_{CIFR} and C_{TIFR} cases, better performance is achieved at higher m, m_s and $\overline{\gamma}$ whereas poor performance is observed at lower m, m_s and $\overline{\gamma}$. The difference in the achievable capacity levels is significant since variations of even greater than 30% are noticed between intense and light

TABLE 3. Exact channel capacity with different adaptation policies under $\mathcal{F}$ fading conditions.

Involved Parameters			Exact Channel Capacity for $A = 2.0$ and $\gamma_0 = \gamma_{\text{th}} = 2$dB				
m	m_s	$\overline{\gamma}$	C_{ORA}, (18)	Ceff, (33)	C_{OPRA}, (52)	C_{CIFR}, (72)	C_{TIFR}, (79)
1.2	1.2	0dB	0.45	0.30	0.09	0.04	0.39
3.2	1.2	0dB	0.48	0.34	0.09	0.16	0.39
3.2	4.2	0dB	0.90	0.75	0.10	0.61	0.63
6.0	6.0	0dB	0.94	0.84	0.06	0.76	0.56
1.2	1.2	10dB	1.76	1.03	0.92	0.35	1.59
3.2	1.2	10dB	1.92	1.27	0.98	1.10	1.67
3.2	4.2	10dB	3.11	2.51	2.22	2.64	2.77
6.0	6.0	10dB	3.25	2.87	2.40	2.99	3.01
1.2	1.2	20dB	4.27	2.39	3.48	1.92	3.32
3.2	1.2	20dB	4.62	3.25	3.84	3.64	3.74
3.2	4.2	20dB	6.22	5.27	5.53	5.74	5.74
6.0	6.0	20dB	6.40	5.89	5.72	6.14	6.14
1.2	1.2	30dB	7.41	4.17	6.72	4.85	5.75
3.2	1.2	30dB	7.84	6.10	7.16	6.85	6.85
3.2	4.2	30dB	9.52	8.47	8.85	9.04	9.04
6.0	6.0	30dB	9.70	9.17	9.04	9.44	9.44
1.2	1.2	40dB	10.71	6.11	10.04	8.12	8.64
3.2	1.2	40dB	11.15	9.31	10.48	10.16	10.16
3.2	4.2	40dB	12.84	11.77	12.17	12.36	12.36
6.0	6.0	40dB	13.02	12.49	12.36	12.76	12.76

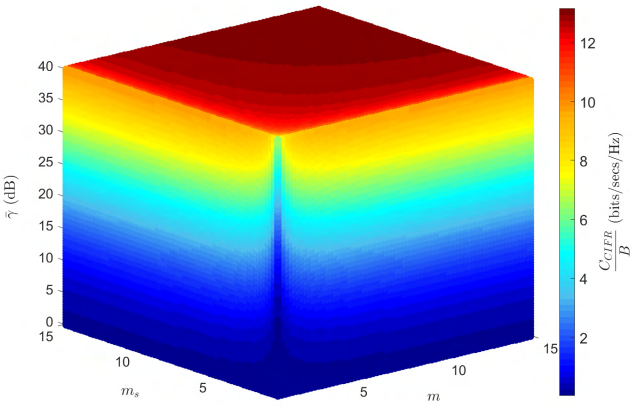

FIGURE 5. C_{CIFR}/B in an $\mathcal{F}$ fading channel as a function of the m, m_s and $\overline{\gamma}$ parameters.

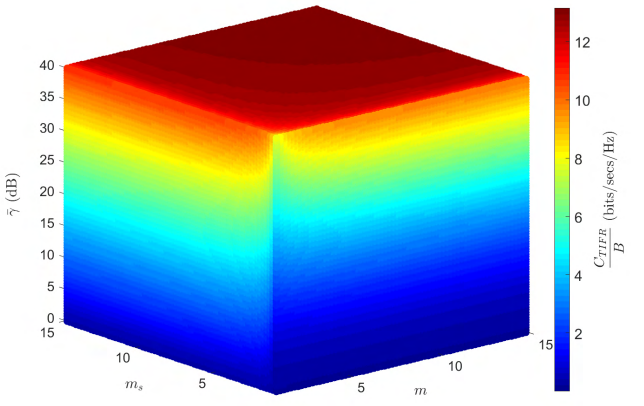

FIGURE 6. C_{TIFR}/B in an $\mathcal{F}$ fading channel as a function of the m, m_s and $\overline{\gamma}$ parameters for $\gamma_0 = 5$ dB.

composite fading conditions across all average SNR regimes. Likewise, Fig. 7 shows the dependence of C_{TIFR}/B on the cutoff SNR, γ_0, for two different fading conditions, i.e., intense and moderate composite fading conditions, and five different average SNR values, namely $\overline{\gamma} = \{0, 10, 20, 30, 40\}$ dB. Furthermore, it is observed that when $\gamma_0 = \gamma_{th}$, the cutoff SNR that maximizes the spectral efficiency (γ_0^*) increases as $\overline{\gamma}$ increases. When comparing Fig. 7(a) and Fig. 7(b), for fixed $\overline{\gamma}$, the value of γ_0^* for the moderate composite fading conditions was greater than that for the intense composite fading conditions. Additionally, for $\gamma_0 < \gamma_0^*$, the curves in Fig. 7(b) are relatively flat compared to that for Fig. 7(a). This verifies that the spectral efficiency improvement provided by truncated channel inversion ($\gamma_0 = \gamma_0^*$), compared to total channel inversion ($\gamma_0 = 0$), is more significant when the channel is subject to severe multipath fading and simultaneous heavy shadowing i.e., intense composite fading conditions.

Table 3 depicts the exact achievable channel capacities for different fading conditions and average SNR values assuming $A = 2$ for C_{eff} and $\gamma_0 = \gamma_{th} = 2$dB for C_{OPRA} and C_{TIFR}. It is shown that the achievable capacities around 0dB are comparable for all types of fading composite fading conditions. However, as the average SNR values increase, we notice larger performance deviations and achievable capacity. Also, the detrimental effect of latency is evident, as this metric exhibits lower performance compared to the other capacity measures. This indicates that latency must be taken into thorough consideration in the determination of the achievable

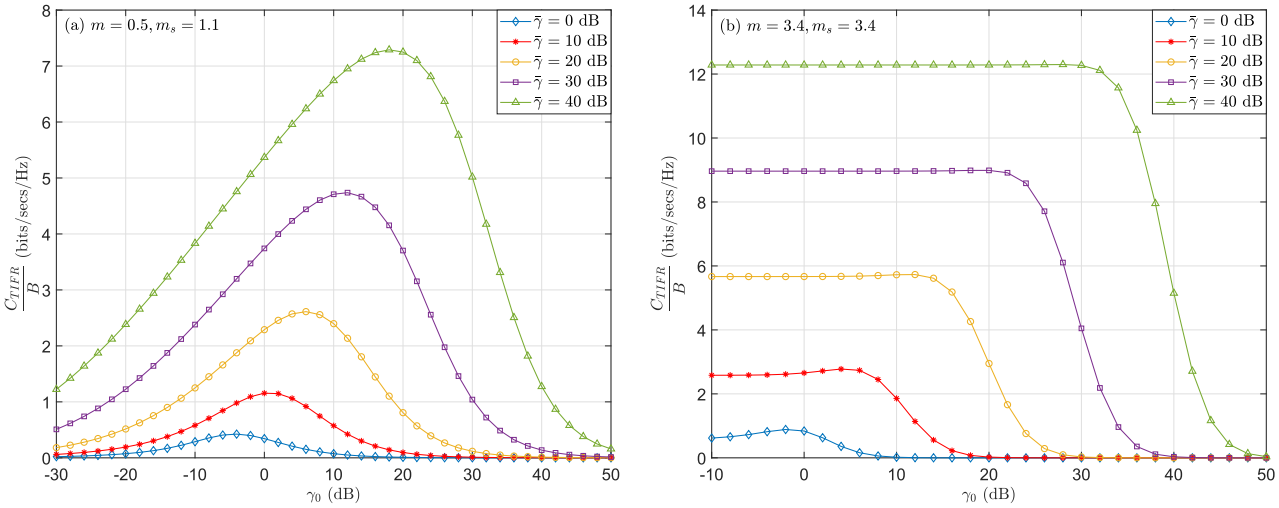

FIGURE 7. C_{TIFR}/B in an $\mathcal{F}$ fading channel as a function of the γ_0 for different $\bar{\gamma}$ values for (a) intense and (b) moderate composite fading conditions.

TABLE 4. Exact and approximate C_{OPRA} and C_{TIFR} for $\gamma_0 = \gamma_{th} = 1$dB.

Involved Parameters			C_{OPRA}		C_{TIFR}	
m	m_s	$\bar{\gamma}$	(52)	(57)	(79)	(98)
2.0	1.5	5dB	0.65	1.42	1.26	0.61
2.0	2.5	5dB	0.89	1.05	1.53	0.96
4.0	2.5	5dB	0.93	0.73	1.58	1.28
2.0	1.5	12dB	2.30	3.51	2.38	1.87
2.0	2.5	12dB	2.86	3.07	2.85	2.53
4.0	2.5	12dB	3.04	2.69	3.07	3.02
2.0	1.5	20dB	4.87	6.11	4.29	4.14
2.0	2.5	20dB	5.49	5.69	5.03	4.95
4.0	2.5	20dB	5.69	5.33	5.52	5.52
2.0	1.5	35dB	9.85	11.10	9.05	9.04
2.0	2.5	35dB	10.48	10.67	9.89	9.89
4.0	2.5	35dB	10.68	10.32	10.48	10.48

performance limits and hence, in the design and deployment of emerging wireless communication systems with stringent quality of service requirements.

Finally, the proposed approximate/bound representations for C_{OPRA} and C_{TIFR} are depicted in Table 4 assuming $\gamma_0 = \gamma_{th} = 1$dB. It is observed that the accuracy/tightness of them is relatively low in the low average SNR regime but their accuracy/tightness increases considerably as the average SNR increases. This is observed across all average SNR regimes and particularly in C_{TIFR}, where the achieved accuracy is significantly high. This verifies the usefulness of these additional analytic representations since they are part of a comprehensive framework that will be useful in future designs and deployments of emerging wireless systems.

VI. CONCLUSION

In this paper, we presented a comprehensive capacity analysis over $\mathcal{F}$ composite fading channels. In particular, it was shown that the tractability of the $\mathcal{F}$ composite fading model led to the determination of the channel capacity for two distinct cases: i) when CSI is available only at the receiver; ii) when CSI is available both at the transmitter and at the receiver. In this context, we derived novel analytic expressions for the capacity of five different schemes, namely (1) optimum rate adaptation; (2) optimum power and rate adaptation; (3) channel inversion with fixed rate; (4) truncated channel inversion with fixed rate; and (5) effective capacity. When comparing these expressions with those for the generalized-K fading channels given in [30], the $\mathcal{F}$ fading model exhibits lower complexity and provides more insights on the impact of the involved parameters on the overall system performance. Based on this, it was shown that the spectral efficiency changes considerably even at slight variations of the average SNR and the severity of the multipath fading and shadowing conditions. The impact of different types of $\mathcal{F}$ composite fading was also investigated through comparisons with the respective capacity for the case of a Rayleigh fading channel. This has highlighted that different types of composite fading can have a profound effect which is beyond the range of the fading conditions experienced in a conventional Rayleigh fading environment. Finally, the new results and insights provided here will be useful in the design and deployment of future communications systems. For example when assessing technologies such as channel selection and spectrum aggregation for use in heterogeneous networks, telemedicine and vehicular communications, to name but a few.

ACKNOWLEDGMENT

This paper was presented in part at the IEEE CommNet 2019, Rabat, Morocco, and the IEEE WCNC 2019, Marrakesh, Morocco.

REFERENCES

[1] H. B. Janes and P. I. Wells, "Some tropospheric scatter propagation measurements near the radio horizon," *Proc. IRE*, vol. 43, no. 10, pp. 1336–1340, Oct. 1955.

[2] S. Basu *et al.*, "250 MHz/GHz scintillation parameters in the equatorial, polar, and auroral environments," *IEEE J. Sel. Areas Commun.*, vol. SAC-5, no. 2, pp. 102–115, Feb. 1987.
[3] S. O. Rice, "Statistical properties of a sine wave plus random noise," *Bell Syst. Tech. J.*, vol. 27, no. 1, pp. 109–157, Jan. 1948.
[4] R. J. C. Bultitude, S. A. Mahmoud, and W. A. Sullivan, "A comparison of indoor radio propagation characteristics at 910 MHz and 1.75 GHz," *IEEE J. Sel. Areas Commun.*, vol. 7, no. 1, pp. 20–30, Jan. 1989.
[5] A. J. Goldsmith and P. P. Varaiya, "Capacity of fading channels with channel side information," *IEEE Trans. Inf. Theory*, vol. 43, no. 6, pp. 1986–1992, Nov. 1997.
[6] M. S. Alouini and A. J. Goldsmith, "Capacity of Rayleigh fading channels under different adaptive transmission and diversity-combining techniques," *IEEE Trans. Veh. Technol.*, vol. 48, no. 4, pp. 1165–1181, Jul. 1999.
[7] M.-S. Alouini and A. J. Goldsmith, "Adaptive modulation over Nakagami fading channels," *Wireless Pers. Commun.*, vol. 13, nos. 1–2, pp. 119–143, May 2000.
[8] Q. T. Zhang and D. P. Liu, "A simple capacity formula for correlated diversity Rician fading channels," *IEEE Commun. Lett.*, vol. 6, no. 11, pp. 481–483, Nov. 2002.
[9] D. B. da Costa and M. D. Yacoub, "Average channel capacity for generalized fading scenarios," *IEEE Commun. Lett.*, vol. 11, no. 12, pp. 949–951, Dec. 2007.
[10] D. B. da Costa and M. D. Yacoub, "Channel capacity for single branch receivers operating in generalized fading scenarios," in *Proc. 4th Int. Symp. Wireless Commun. Syst.*, Oct. 2007, pp. 215–218.
[11] P. S. Bithas and P. T. Mathiopoulos, "Capacity of correlated generalized gamma fading with dual-branch selection diversity," *IEEE Trans. Veh. Technol.*, vol. 58, no. 9, pp. 5258–5663, Nov. 2009.
[12] P. S. Bithas, G. P. Efthymoglou, and N. C. Sagias, "Spectral efficiency of adaptive transmission and selection diversity on generalised fading channels," *IET Commun.*, vol. 4, no. 17, pp. 2058–2064, Nov. 2010.
[13] M. Matthaiou, N. D. Chatzidiamantis, and G. K. Karagiannidis, "A new lower bound on the ergodic capacity of distributed MIMO systems," *IEEE Signal Process. Lett.*, vol. 18, no. 4, pp. 227–230, Apr. 2011.
[14] J. Zhang, Z. Tan, H. Wang, Q. Huang, and L. Hanzo, "The effective throughput of MISO systems over κ-μ fading channels," *IEEE Trans. Veh. Technol.*, vol. 63, no. 2, pp. 943–947, Feb. 2014.
[15] H. Hashemi, "The indoor radio propagation channel," *Proc. IEEE*, vol. 81, no. 7, pp. 943–968, Jul. 1993.
[16] J. R. Clark and S. Karp, "Approximations for lognormally fading optical signals," *Proc. IEEE*, vol. 58, no. 12, pp. 1964–1965, Dec. 1970.
[17] A. Abdi and M. Kaveh, "On the utility of gamma PDF in modeling shadow fading (slow fading)," in *Proc. IEEE 49th Veh. Technol. Conf.*, vol. 3, May 1999, pp. 2308–2312.
[18] A. H. Marcus, "Power sum distributions: An easier approach using the wald distribution," *J. Amer. Stat. Assoc.*, vol. 71, no. 353, pp. 237–238, Apr. 1976.
[19] H. G. Sandalidis, N. D. Chatzidiamantis, and G. K. Karagiannidis, "A tractable model for turbulence- and misalignment-induced fading in optical wireless systems," *IEEE Commun. Lett.*, vol. 20, no. 9, pp. 1904–1907, Sep. 2016.
[20] I. Trigui, A. Laourine, S. Affes, and A. Stéphenne, "The inverse Gaussian distribution in wireless channels: Second-order statistics and channel capacity," *IEEE Trans. Commun.*, vol. 60, no. 11, pp. 3167–3173, Nov. 2012.
[21] A. Abdi and M. Kaveh, "*K* distribution: An appropriate substitute for Rayleigh-lognormal distribution in fading-shadowing wireless channels," *IET Electron. Lett.*, vol. 34, no. 9, pp. 851–852, Apr. 1998.
[22] A. Abdi, W. C. Lau, M.-S. Alouini, and M. Kaveh, "A new simple model for land mobile satellite channels: First- and second-order statistics," *IEEE Trans. Wireless Commun.*, vol. 2, no. 3, pp. 519–528, May 2003.
[23] H. Suzuki, "A statistical model for urban radio propogation," *IEEE Trans. Commun.*, vol. 25, no. 7, pp. 673–680, Jul. 1977.
[24] G. E. Corazza and F. Vatalaro, "A statistical model for land mobile satellite channels and its application to nongeostationary orbit systems," *IEEE Trans. Veh. Technol.*, vol. 43, no. 3, pp. 738–742, Aug. 1994.
[25] I. M. Kostić, "Analytical approach to performance analysis for channel subject to shadowing and fading," *IEE Proc.-Commun.*, vol. 152, no. 6, pp. 821–827, Dec. 2005.
[26] R. Agrawal, "On efficacy of Rayleigh-inverse Gaussian distribution over *K*-distribution for wireless fading channels," *Wireless Commun. Mobile Comput.*, vol. 7, no. 1, pp. 1–7, Jan. 2007.
[27] P. S. Bithas, "Weibull-gamma composite distribution: Alternative multipath/shadowing fading model," *IET Electron. Lett.*, vol. 45, no. 14, pp. 749–751, Jul. 2009.
[28] P. C. Sofotasios, T. A. Tsiftsis, M. Ghogho, L. R. Wilhelmsson, and M. Valkama, "The η-μ / *IG* distribution: A novel physical multipath/shadowing fading model," in *Proc. IEEE Int. Conf. Commun. (ICC)*, Jun. 2013, pp. 5715–5719.
[29] A. Abdi and M. Kaveh, "Comparison of DPSK and MSK bit error rates for *K* and Rayleigh-lognormal fading distributions," *IEEE Commun. Lett.*, vol. 4, no. 4, pp. 122–124, Apr. 2000.
[30] A. Laourine, M.-S. Alouini, S. Affes, and A. Stéphenne, "On the capacity of generalized-*K* fading channels," *IEEE Trans. Wireless Commun.*, vol. 7, no. 7, pp. 2441–2445, Jul. 2008.
[31] F. Yilmaz and M.-S. Alouini, "A new simple model for composite fading channels: Second order statistics and channel capacity," in *Proc. 7th Int. Symp. Wireless Commun. Syst. (ISWC)*, Sep. 2010, pp. 676–680.
[32] P. S. Bithas, N. C. Sagias, P. T. Mathiopoulos, G. K. Karagiannidis, and A. A. Rontogiannis, "On the performance analysis of digital communications over generalized-*K* fading channels," *IEEE Commun. Lett.*, vol. 10, no. 5, pp. 353–355, May 2006.
[33] L. Moreno-Pozas, F. J. Lopez-Martinez, J. F. Paris, and E. Martos-Naya, "The κ-μ shadowed fading model: Unifying the κ-μ and η-μ distributions," *IEEE Trans. Veh. Technol.*, vol. 65, no. 12, pp. 9630–9641, Dec. 2016.
[34] J. F. Paris, "Statistical characterization of κ-μ shadowed fading," *IEEE Trans. Veh. Technol.*, vol. 63, no. 2, pp. 518–526, Feb. 2014.
[35] M. C. Clemente and J. F. Paris, "Closed-form statistics for sum of squared Rician shadowed variates and its application, *IET Electron. Lett.*, vol. 50, no. 2, pp. 120–121, Jan. 2014.
[36] P. S. Bithas, N. C. Sagias, P. T. Mathiopoulos, S. A. Kotsopoulos, and A. M. Maras, "On the correlated *K*-distribution with arbitrary fading parameters," *IEEE Signal Process. Lett.*, vol. 15, no. 7, pp. 541–544, Jul. 2008.
[37] J. Zhang, M. Matthaiou, Z. Tan, and H. Wang, "Performance analysis of digital communication systems over composite η-μ/gamma fading channels," *IEEE Trans. Veh. Technol.*, vol. 61, no. 7, pp. 3114–3124, Sep. 2012.
[38] N. D. Chatzidiamantis and G. K. Karagiannidis, "On the distribution of the sum of gamma-gamma variates and applications in RF and optical wireless communications," *IEEE Trans. Commun.*, vol. 59, no. 5, pp. 1298–1308, May 2011.
[39] M. Matthaiou, N. D. Chatzidiamantis, G. K. Karagiannidis, and J. A. Nossek, "On the capacity of generalized-*K* fading MIMO channels," *IEEE Trans. Signal Process.*, vol. 58, no. 11, pp. 5939–5944, Nov. 2010.
[40] M. Matthaiou, N. D. Chatzidiamantis, G. K. Karagiannidis, and J. A. Nossek, "ZF detectors over correlated *K* fading MIMO channels," *IEEE Trans. Commun.*, vol. 59, no. 6, pp. 1591–1603, Jun. 2011.
[41] C. Zhong, M. Matthaiou, G. K. Karagiannidis, A. Huang, and Z. Zhang, "Capacity bounds for AF dual-hop relaying in *G* fading channels," *IEEE Trans. Veh. Technol.*, vol. 61, no. 4, pp. 1730–1740, May 2012.
[42] X. Li, J. Li, L. Li, J. Jin, J. Zhang, and D. Zhangm, "Effective rate of MISO systems over κ-μ shadowed fading channels," *IEEE Access*, vol. 5, no. 3, pp. 10605–10611, 2017.
[43] M. You, H. Sun, J. Jiang, and J. Zhang, "Unified framework for the effective rate analysis of wireless communication systems over MISO fading channels," *IEEE Trans. Commun.*, vol. 65, no. 4, pp. 1775–1785 Apr. 2017.
[44] J. Zhang, L. Dai, W. H. Gerstacker, and Z. Wang, "Effective capacity of communication systems over κ-μ shadowed fading channels," *IET Electron. Lett.*, vol. 51, no. 19, pp. 1540–1542, Jul. 2015.
[45] K. P. Peppas, P. T. Mathiopoulos, and J. Yang, "On the effective capacity of amplify-and-forward multihop transmission over arbitrary and correlated fading channels," *IEEE Wireless Commun. Lett.*, vol. 5, no. 3, pp. 248–251, Jun. 2016.
[46] A. Laourine, M.-S. Alouini, S. Affes, and A. Stéphenne, "On the performance analysis of composite multipath/shadowing channels using the *G*-distribution," *IEEE Trans. Commun.*, vol. 57, no. 4, pp. 5715–5719, Apr. 2009.
[47] F. S. Almehmadi and O. S. Badarneh, "On the effective capacity of Fisher–Snedecor *F* fading channels," *IET Electron. Lett.*, vol. 54, no. 18, pp. 1068–1070, Sep. 2018.
[48] S. Chen, J. Zhang, G. K. Karagiannidis, and B. Ai, "Effective rate of MISO systems over Fisher–Snedecor *F* fading channels," *IEEE Commun. Lett.*, vol. 22, no. 12, pp. 2619–2622, Dec. 2018.

[49] S. K. Yoo, S. L. Cotton, P. C. Sofotasios, M. Matthaiou, M. Valkama, and G. K. Karagiannidis, "The Fisher-Snedecor F distribution: A simple and accurate composite fading model," *IEEE Commun. Lett.*, vol. 21, no. 7, pp. 1661–1664, Jul. 2017.

[50] M. Nakagami, *The m-Distribution: A General Formula of Intensity Distribution of Rapid Fading*. Amsterdam, The Netherlands: Elsevier, 1960.

[51] I. S. Gradshteyn and I. M. Ryzhik, *Table of Integrals, Series, and Products*, 7th ed. London, U.K.: Academic Press, 2007.

[52] M. K. Simon and M.-S. Alouini, *Digital Communication Over Fading Channels*, 2nd ed. New York, NY, USA: Wiley, 2005.

[53] A. P. Prudnikov, Y. A. Brychkov, and O. I. Marichev, *Integrals and Series: Elementary Functions*, vol. 1, 3rd ed. New York, NY, USA: Gordon and Breach Science, 1992.

[54] F. Yilmaz and M.-S. Alouini, "Novel asymptotic results on the high-order statistics of the channel capacity over generalized fading channels," in *Proc. IEEE 13th Int. Workshop Signal Process. Adv. Wireless Commun. (SPAWC)*, Cesme, Turkey, Jun. 2012, pp. 389–393.

[55] I. S. Ansari, M.-S. Alouini, and J. Cheng, "On the capacity of FSO links under lognormal and rician-lognormal turbulences," in *Proc. IEEE 80th Veh. Technol. Conf. (VTC Fall)*, Vancouver, BC, Canada, Sep. 2014, pp. 1–6.

[56] Z. Ji, C. Dong, Y. Wang, and J. Lu, "On the analysis of effective capacity over generalized fading channels," in *Proc. IEEE Int. Conf. Commun. (ICC)*, Sydney, NSW, Australia, Jun. 2014, pp. 1977–1983.

[57] J. Zhang, L. Dai, Z. Wang, D. W. K. Ng, and W. H. Gerstacker, "Effective rate analysis of MISO systems over α-μ fading channels," in *Proc. IEEE Global Commun. Conf. (GLOBECOM)*, San Diego, CA, USA, Dec. 2015, pp. 1–6.

SEONG KI YOO (S'14–M'17) received the B.Eng. degree (Hons.) in telecommunication systems from the University of Surrey, Guildford, U.K., in 2010, the M.Sc. degree in communications and signal processing from Imperial College London, London, U.K., in 2012, and the Ph.D. degree from Queen's University Belfast, Belfast, U.K., in 2017.

He was a Junior Researcher with the Korea Electrotechnology Research Institute, Ansan, South Korea, from 2012 to 2013. He is currently a Postdoctoral Research Fellow with the Centre for Wireless Innovation, ECIT Institute, Queen's University Belfast. His research interests include the areas of fading channel characterization and modeling for wearable communications and diversity in wearable applications. His doctoral studies were supported sponsored by U.K. EPSRC.

PASCHALIS C. SOFOTASIOS (S'07–M'12–SM'16) was born in Volos, Greece, in 1978. He received the M.Eng. degree from Newcastle University, U.K., in 2004, the M.Sc. degree from the University of Surrey, U.K., in 2006, and the Ph.D. degree from the University of Leeds, U.K., in 2011. His M.Sc. degree was supported by a scholarship from U.K.-EPSRC and his Ph.D. degree supported by U.K.-EPSRC and Pace plc. He has held academic positions at the University of Leeds, U.K., the University of California at Los Angeles, Los Angeles, USA, the Aristotle University of Thessaloniki, Greece, Tampere University of Technology, Finland, and Khalifa University, United Arab Emirates, where he is currently an Assistant Professor. His research interests include the broad areas of digital and optical wireless communications, including topics on pure mathematics and statistics.

Dr. Sofotasios has been a member and the Co-Chair of the Technical Program Committee of numerous IEEE conferences. He has received an Exemplary Reviewer Award for the IEEE COMMUNICATIONS LETTERS, in 2012, and the IEEE TRANSACTIONS ON COMMUNICATIONS, in 2015 and 2016. He was a co-recipient of the Best Paper Award from ICUFN 2013. He currently serves as an Editor for the IEEE COMMUNICATIONS LETTERS.

SIMON L. COTTON (S'04–M'07–SM'14) received the B.Eng. degree in electronics and software from the University of Ulster, Ulster, U.K., in 2004, and the Ph.D. degree in electrical and electronic engineering from Queen's University Belfast, Belfast, U.K., in 2007. He is currently a Reader in wireless communications with the Institute of Electronics, Communications, and Information Technology, Queen's University Belfast. He is also the Co-Founder and the Chief Technology Officer with ActivWireless Ltd., Belfast. He has authored or co-authored over 100 publications in major IEEE/IET journals and refereed international conferences, and two book chapters. He holds two patents. His research interests include cellular device-to-device, vehicular, and wearable communications, radio channel characterization and modeling, and the simulation of wireless channels.

Dr. Cotton has received the H. A. Wheeler Prize from the IEEE Antennas and Propagation Society, in 2010, for the best applications journal paper in the IEEE TRANSACTIONS ON ANTENNAS AND PROPAGATION in 2009. In 2011, he has received the Sir George Macfarlane Award from the U.K. Royal Academy of Engineering in recognition of his technical and scientific attainment since graduating from his first degree in engineering.

SAMI MUHAIDAT (S'01–M'07–SM'11) received the Ph.D. degree in electrical and computer engineering from the University of Waterloo, Waterloo, ON, Canada, in 2006. From 2007 to 2008, he was an NSERC Postdoctoral Fellow with the Department of Electrical and Computer Engineering, University of Toronto, Canada. From 2008 to 2012, he was an Assistant Professor with the School of Engineering Science, Simon Fraser University, Burnaby, BC, Canada. He is currently an Associate Professor with Khalifa University, and a Visiting Reader (Associate Professor) with the Faculty of Engineering, University of Surrey, U.K. His research focuses on wireless communications, optical communications, the IoT with emphasis on battery-less devices, and machine learning. He is also a member of the Mohammed Bin Rashid Academy of Scientists. He is currently an Area Editor of the IEEE TRANSACTIONS ON COMMUNICATIONS. He has served as a Senior Editor for the IEEE COMMUNICATIONS LETTERS, an Editor for the IEEE TRANSACTIONS ON COMMUNICATIONS, and an Associate Editor for the IEEE TRANSACTIONS ON VEHICULAR TECHNOLOGY.

F. JAVIER LOPEZ-MARTINEZ (SM'17) received the M.Sc. and Ph.D. degrees in telecommunication engineering from the Universidad de Málaga, Spain, in 2005 and 2010, respectively. He joined the Communication Engineering Department, Universidad de Málaga, in 2005, as an Associate Researcher, where he has been an Assistant Professor, since 2015. He was a Marie Curie Postdoctoral Fellow with Wireless Systems Lab, Stanford University, from 2012 to 2014, and the Universidad de Málaga, from 2014 to 2015. He has been a Visiting Researcher with University College London, since 2010, and Queen's University Belfast, since 2018. His research interests include a diverse set of topics in the wide areas of communication theory and wireless communications, including stochastic processes, wireless channel modeling, random matrix theory, physical layer security, and wireless powered communications.

Dr. Lopez-Martinez has received several research awards, including the Best Paper Award from the Communication Theory Symposium at the IEEE GLOBECOM 2013, the IEEE COMMUNICATIONS LETTERS Exemplary Reviewer Certificate in 2014, and the IEEE TRANSACTIONS ON COMMUNICATIONS Exemplary Reviewer Certificate in 2015 and 2017. He is an Editor of the IEEE TRANSACTIONS ON COMMUNICATIONS, in the area of wireless communications.

JUAN M. ROMERO-JEREZ (SM'14) received the M.Sc. degree in telecommunication engineering and mathematics and the Ph.D. degree in telecommunication engineering from the Universidad de Málaga, Spain, in 2001.

In 1996, he joined the Electronic Technology Department, Universidad de Málaga, where he has been an Associate Professor, since 2002. He was a Visiting Associate Professor with the Electrical Engineering Department, Stanford University, from 2005 to 2006, from 2007 to 2008, and in 2016. He has participated in several research projects in the areas of packet radio transmission, multiple antennas, interference management, and cellular networks. His current research interest includes the area of wireless communications, more specifically wireless communications performance analysis, multipath fading, wireless channel modeling, diversity systems, smart antennas, MIMO performance, and interference management. He is an Editor of the IEEE TRANSACTIONS ON WIRELESS COMMUNICATIONS.

GEORGE K. KARAGIANNIDIS (M'96–SM'03–F'14) was born in Pithagorion, Greece. He received the Diploma and Ph.D. degree in electrical and computer engineering from the University of Patras, in 1987 and 1999, respectively.

From 2000 to 2004, he was a Senior Researcher with the Institute for Space Applications and Remote Sensing, National Observatory of Athens, Greece. In 2004, he joined the Aristotle University of Thessaloniki, Greece, as a Faculty Member, where he is currently a Professor with the Electrical and Computer Engineering Department and the Director of the Digital Telecommunications Systems and Networks Laboratory. He is also an Honorary Professor with Southwest Jiaotong University, Chengdu, China. He is a highly cited author across all areas of electrical engineering, and he has been recognized as a Thomson Reuters Highly Cited Researcher, since 2019. He has authored or co-authored over 400 technical papers published in scientific journals and presented at international conferences. He has also authored the Greek edition of a book *Telecommunications Systems*, and he has co-authored the book *Advanced Optical Wireless Communications Systems* (Cambridge University Press, 2012). His research interests include the broad areas of digital communications systems and signal processing, with emphasis on wireless communications, optical wireless communications, wireless power transfer and its applications, molecular communications, communications and robotics, and wireless security. He has been the General Chair, the Technical Program Chair, and a member of Technical Program Committee in several IEEE and non-IEEE conferences. He was an Editor of the IEEE TRANSACTIONS ON COMMUNICATIONS, a Senior Editor of the IEEE COMMUNICATIONS LETTERS, an Editor of the *EURASIP Journal of Wireless Communications and Networking*, and several times a Guest Editor of the IEEE SELECTED AREAS IN COMMUNICATIONS. From 2012 to 2015, he was the Editor-in-Chief of the IEEE COMMUNICATIONS LETTERS.